

Article

# Morphostructural, Meteorological and Seismic Factors Controlling Landslides in Weak Rocks: The Case Studies of Castelnuovo and Ponzano (North East Abruzzo, Central Italy)

Monia Calista <sup>1</sup>, Enrico Miccadei <sup>1,2,\*</sup>  and Nicola Sciarra <sup>1</sup>

<sup>1</sup> Department of Engineering and Geology, Università degli Studi “G. d’Annunzio” Chieti-Pescara, Via dei Vestini 31, 66100 Chieti Scalo (CH), Italy; monia.calista@unich.it (M.C.); enrico.miccadei@unich.it (E.M.); nicola.sciarra@unich.it (N.S.)

<sup>2</sup> Istituto Nazionale di Geofisica e Vulcanologia, Sezione Roma 1, Via di Vigna Murata 605, 00143 Rome, Italy

\* Correspondence: tommaso.piacentini@unich.it; Tel.: +39-0871-355-6422

Received: 6 January 2019; Accepted: 4 March 2019; Published: 9 March 2019



**Abstract:** We investigated the role of the morphostructural setting and seismic and meteorological factors in the development of landslides in the piedmont of the Abruzzo Apennines. In February 2017, following a heavy snow precipitation event and a moderate seismic sequence (at the end of the Central Italy 2016–2017 seismic crisis), several landslides affected the NE-Abruzzo chain and piedmont area. This work is focused on the Ponzano landslide (Civitella del Tronto, Teramo) and the Castelnuovo landslide (Campoli, Teramo) in the NE Abruzzo hilly piedmont. These landslides consist of: (1) a large translational slide-complex landslide, affecting the Miocene–Pliocene sandstone clay bedrock sequence of the piedmont hilly sector; and (2) a complex (topple/fall-slide) landslide, which occurred along a high and steep scarp on conglomerate rocks pertaining to terraced alluvial fan deposits of the Pleistocene superficial deposits. Both of the landslides are typical of the Abruzzo hilly piedmont and both of them largely affected houses and villages located on top of the scarp or within the slope. The landslides were studied by means of field geological and geomorphological mapping, borehole investigations, geostructural analysis and photogeological analysis. For the Ponzano landslide, a detail pre-post-landslide air photo interpretation allowed for defining the deformation pattern occurred on the slope. For the Castelnuovo landslide, the triggering factors and the stability of the slope were evaluated with FLAC3D numerical modelling, in pre- and post-landslide conditions. Through this integrated analysis, the triggering factors, the landslide mechanism and the stability conditions of the landslides and the characterization of two main types of landslides affecting the piedmont hilly area of the Abruzzo region were investigated.

**Keywords:** landslides; rainfall; snowfall; morphostructural setting; seismicity; Abruzzo hilly area

## 1. Introduction

Landsliding is one of the main processes inducing geomorphological changes on slopes in mountainous, hilly and coastal areas. Landslides are controlled by several predisposing factors (i.e., morphology, lithology, structural setting, vegetation, land use, climate, etc.) and are induced by different triggering factors (e.g., heavy rainfall and snowfall events, snow melting, earthquakes, sea storms, etc.) [1–7]. When affecting soft and weak rocks, landslides are also largely dependent on the morphostructural setting of the rocks and/or on the main jointing affecting the rock masses. The investigation of these factors and of the mechanism/evolution of the landslides is necessary in different morphostructural domains for the assessment of the areas prone to landslides and of their

triggering during heavy meteorological and/or seismic events. Moreover, the possibility of a causal link between seismic events and the triggering of landslides should be investigated, both when landslide phenomena are concomitant and delayed over a period of even weeks [6–12]. This investigation should be based on the integration of different approaches (e.g., detailed geological and geomorphological survey, geomechanical survey, subsurface direct-indirect investigations, remote sensing, numerical modelling, etc.) [3,7,13–16].

In January 2017, the Abruzzo region, in the eastern side of Central Italy, was affected by a heavy snow precipitation event (up to >3 m in the mountain area and 1–1.5 m in the hilly piedmont) [17,18] and by the last strong earthquakes ( $M_w > 5$ ) of the 2016–2017 seismic crisis of the central Apennines (National Institute of Geophysics and Volcanology [INGV] [19,20]). After this combination of seismic and meteorological events, from January to February 2017, several avalanches, landslides and flooding events occurred in the Abruzzo area, particularly in the NE piedmont hilly area from the Apennines chain to the Adriatic coast (Figures 1 and 2). These events caused severe damage and many casualties and evacuees and were declared an official natural disaster at regional government level [17]. These types of events have occurred repeatedly in the last decades in the Abruzzo area as well as all around Italy and are expected to increase in the next years in connection with climate changes [7–9,21] and deserve detailed/integrated investigations both at local and at regional level.

This work used an integrated geomorphological analysis for the investigation of two main landslide cases in the piedmont hilly area of NE-Abruzzo (at ~40–45 km from the January 2017 earthquakes epicentres): the Ponzano landslide on 12 February 2017 (Civitella del Tronto, Teramo) and the Castelnuovo landslide on 16 February 2017 (Campoli, Teramo) (Figure 2). These landslide events, as well as those, occurred in January–February 2017 (Figure 2), were controlled by a combination of morphologic and litho-structural predisposing factors and induced by meteorological (e.g., rainfall, snowfall, snowmelt) and possibly connected to the previous seismicity. The Ponzano landslide affected the Miocene–Pliocene pelitic-arenaceous bedrock sequence of the Adriatic piedmont hilly sector with a mainly translational sliding mechanism. In the upper-middle part of the landslides, several houses of Ponzano village were heavily damaged, inducing their evacuation [22,23]. The Castelnuovo area is characterized by tabular relief on moderately consistent and jointed terraced alluvial fan deposits covering the bedrock. The southern side of the tabular relief was affected by a complex landslide. As occurred several times in the last centuries [24], this landslide involved the urban area of the village; one building was heavily damaged and several houses very close to the main scarp were evacuated. The Ponzano and Castelnuovo cases were selected as largely representative of the main landslide types affecting the different morphostructural setting of the Adriatic piedmont [25,26] and for the analysis with different integrated approaches according to different types of landslides. The analysis of these cases is based on an interdisciplinary investigation incorporating field geological and geomorphological mapping, geostructural analysis, photogeological analysis (unmanned aerial vehicle UAV images and orthophoto), borehole investigation and numerical modelling. This allowed the landslide failure kinematics and the main controlling factors (e.g., lithological, structural, meteorological, seismic, etc.) to be inferred. For the Ponzano landslide, a detailed pre-post-landslide air-photo interpretation allowed for defining the distribution of the deformation occurred on the slope. For the Castelnuovo case, since the landslide was sudden and fast, the failure kinematics and the predisposing/triggering factors were also analysed by means of numerical modelling for stability analysis. Both the pre-landslide and post-landslide slope models were analysed. The pre-landslide one allowed for the investigation of the landslide triggering and failure kinematics, while the post-landslide one supported the investigation of the current stability conditions and expected future landslides.

The modelling of complex gravitational phenomena is based on the study of the geotechnical behaviour of a 3D soil/rock moving mass, which assumes more relevant interest than classical stability analysis methods. Numerical methods allow the investigation of the deformative behaviour both of rigid blocks [27–29] and ductile masses [30,31] providing a broader definition of the evolutionary process. In the numerical modelling, a soil/rock mass is considered a complex system, resulting

for example from weathering (see among many others [32]) and erosion, studied through either Computational Fluid Dynamics or the more simplified but effective Cellular Automata tool [33], supplemented by closure laws [34]. This would require statistical approaches, considering the possible numerical values of the geotechnical parameters as random variables [35–37]. However, in order to simplify the simulations, we adopted a deterministic approach aimed at characterizing the numerical values of the selected geomechanical parameters. For the purpose of this work, we have selected the FLAC family computer code, in its 3D version. It is based on Finite Difference Method applied to continuum mechanics (among many others [38]) and is widely used for slope stability studies, in which the slope is generally analysed as a continuous [39,40]. In this work, the slope was instead considered as a complex geological volume, including the main discontinuities resulting from the geomorphological-structural analysis, inserted in order to evaluate their influence on landslide mechanism. Moreover, adding the pore water pressures, the numerical modelling allowed to simulate the water infiltration (after rainfall and snowmelt). Finally, the influence of the earthquake was evaluated. In order to consider such dynamic effects, it is possible to insert both sinusoidal seismic waves at different frequencies and real accelerograms [41,42]. In our case, real accelerograms were used in the model.

The integration of different types of investigations has allowed us to reconstruct a geological and geomorphological model of the Ponzano and Castelnuovo landslides and to characterize mechanisms and factors that have controlled their evolution in different orographic, geological and morphostructural conditions. Through these case studies, the landslide events that occurred in NE-Abruzzo in January–February 2017 after seismic and meteorological heavy events were characterized, focusing on the triggering/predisposing factors, the landslide mechanism in connection to the morphostructural setting and the current stability conditions. Since earthquakes and meteorological events occurred several times in the last decades in Abruzzo and all over Italy, this work provides a contribution, in terms of local case studies, factors/mechanisms investigation, for the understanding of the landslides largely and repeatedly affecting the piedmont hilly area of the Apennines.

## 2. Study Areas

### 2.1. Regional Setting of the Apennine Piedmont Hilly Area of NE-Abruzzo

#### 2.1.1. Morphostructural Setting

The study areas are located in the piedmont of the Central Apennines in the NE-Abruzzo region (Figure 1) between the Tordino River and the Salinello River. The front of the chain is located along the Montagna dei Fiori ridge and the Gran Sasso ridge and drops down to the piedmont area. This sector, as well as the entire Adriatic piedmont, shows a cuesta, mesa and plateau landscape resulting from the evolution of the Adriatic foredeep domain of the Apennine orogenic system [43–46]. The elevation ranges from 0 m to ~600 m a.s.l. along the main drainage divides between the main rivers and the terrain gradient (derived from a 10 m cell digital elevation model [DEM] [47]) ranges from flat along the river and coastal plains to  $>40^\circ$  with local vertical scarps along the slopes. From the mountain area to the piedmont, the landscape is carved by the main river valleys (featuring fluvial plains up to 4 km in width), roughly perpendicular to the coast and by minor catchments flowing toward the main valleys and the coastal plain (featuring radial, trellis and angular drainage patterns) [25,48]. The coastal area is characterized by wide coastal slopes and a coastal plain up to  $>1$  km in width [49].

The bedrock consists of a sequence of marine pelitic-arenaceous rocks (Upper Miocene–Lower Pliocene) arranged in a fold and thrust setting, affected by regional NNW-SSE oriented Pliocene thrusts and high-angle normal faults, which are still connected to active moderate seismicity. It is overlain by a sequence of marine clayey-sandy-conglomeratic rocks (Upper Pliocene–Lower Pleistocene) in a gently NE-dipping homoclinal setting. Patches of travertine deposits and entrenched fluvial and alluvial fan

deposits, as well as slope, colluvial and landslide superficial deposits (Middle Pleistocene–Holocene) extensively cover the bedrock [25,50–55] (Figure 2).

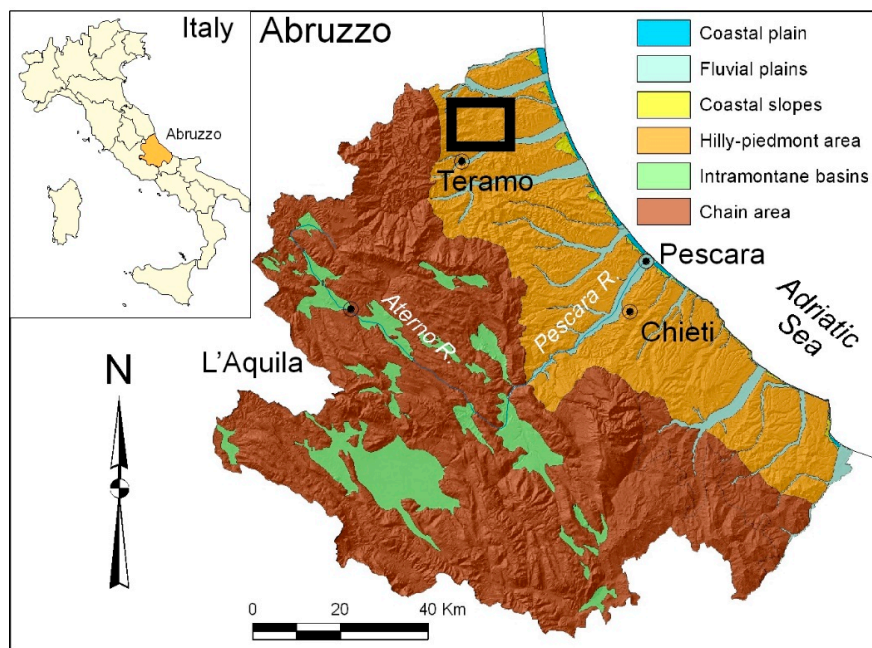


**Figure 1.** Location map and main physiographic domains of the Abruzzo region (the study areas are in the black box).

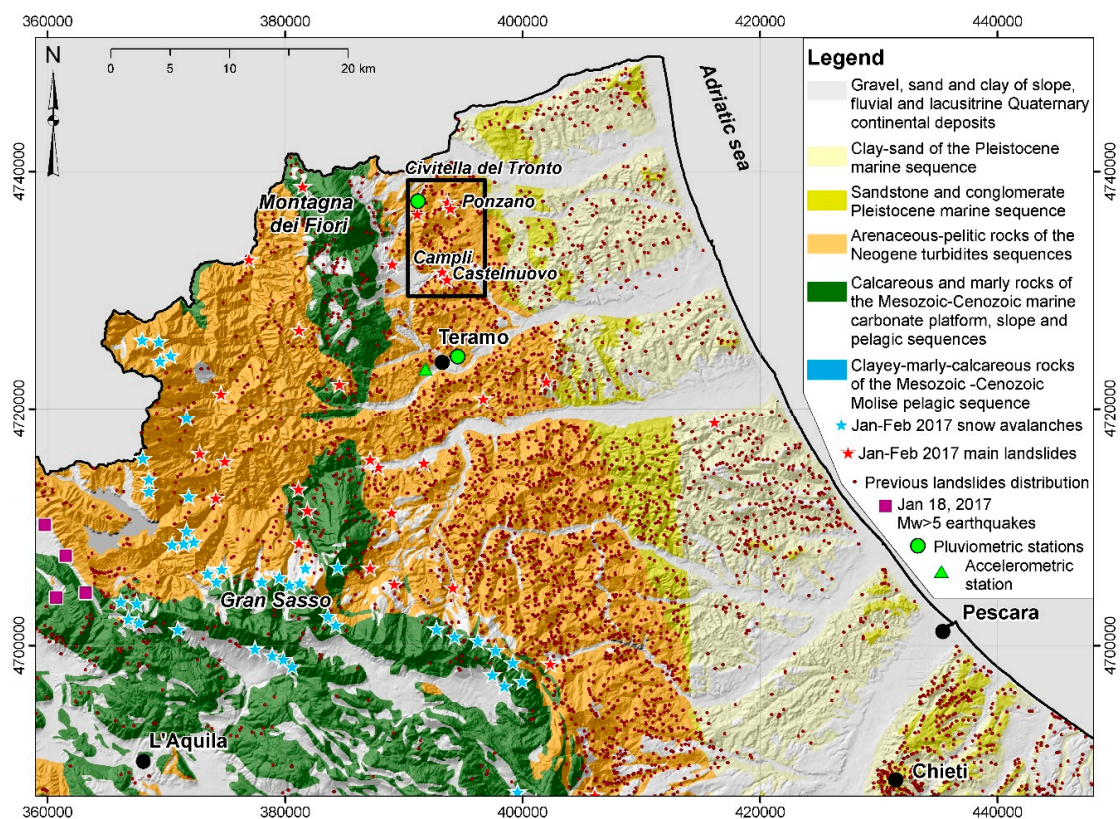


**Figure 2.** Lithological scheme of the NE-Abruzzo region and distribution of the main landslides. The study area is in the black box. Previous landslides derived from IFFI Project [26]; January–February 2017 avalanches and landslides provided by Protezione Civile Abruzzo Region and from local chronicles and field survey.

The piedmont-coastal hilly landscape is incised by approximately WSW–ENE-oriented consequent valleys (i.e., the Salinello valley and the Tordino valley) that are characterized by fluvial deposits arranged in flights of at least four orders of terraces (Middle Pleistocene–Holocene) [52–54]. The valley sides, as well as the coastal slopes, are extensively affected by different types of landslides (e.g., mostly rotational-translational slides, flow, complex slides) [26,49,55,56].

The geomorphologic processes are mainly fluvial, gravity-induced and mass wasting. These processes are frequently activated by the heavy rainfall events that affect the region and by seismic events. Fluvial processes affect the main rivers, alternating channel incisions and flooding. The slope processes due to running water mostly affect the clayey and pelitic-arenaceous hills of piedmont and the coastal areas, generating badlands and minor landforms such as rills, gullies and mudflows [54,57]. Mass-wasting processes have induced the formation of a widespread landslides and mass movements, mostly affecting the hilly piedmont area and the coastal area [1,26,49,56,58].

### 2.1.2. Climate and Meteorological Features

The Abruzzo climate is generally Mediterranean type. However, it is largely affected by the orography, changing from a Mediterranean type with maritime influence along the coasts and in the piedmont hilly area to more continental-like in the inland Abruzzo region [59]. The rainfall distribution is also controlled by the relief arrangement; the highest annual rainfall values (up to 1500–2000 mm/year) occur along the main ridges and on the west-exposed mountainsides, while the annual rainfall decreases down to ~600 mm/year along the Adriatic coast. The hilly piedmont-coastal area is characterized by a maritime Mediterranean climate [60]. The average annual precipitation is 600–800 mm/year, with occasional heavy rainfall (>100 mm/d and 30–40 mm/h) [21,61]. In recent decades, this area has been affected by flash flood events, which were induced by heavy rainfall ranging from 60–80 mm in a few hours to >200 mm in one day (e.g., January 2003, October 2007, March 2011, September 2012, December 2013, February–March 2015, January–February 2017 [21]).

In the first months of 2017, Abruzzo was affected by intense snowfall and rainfall. In January 2017, cold currents from the Balkans caused an abrupt decrease in temperature (Figure 3), causing up to 2–3 m of snow cover from the main eastern Abruzzo ridges down to the coastal areas (1–1.5 m in the hilly piedmont).

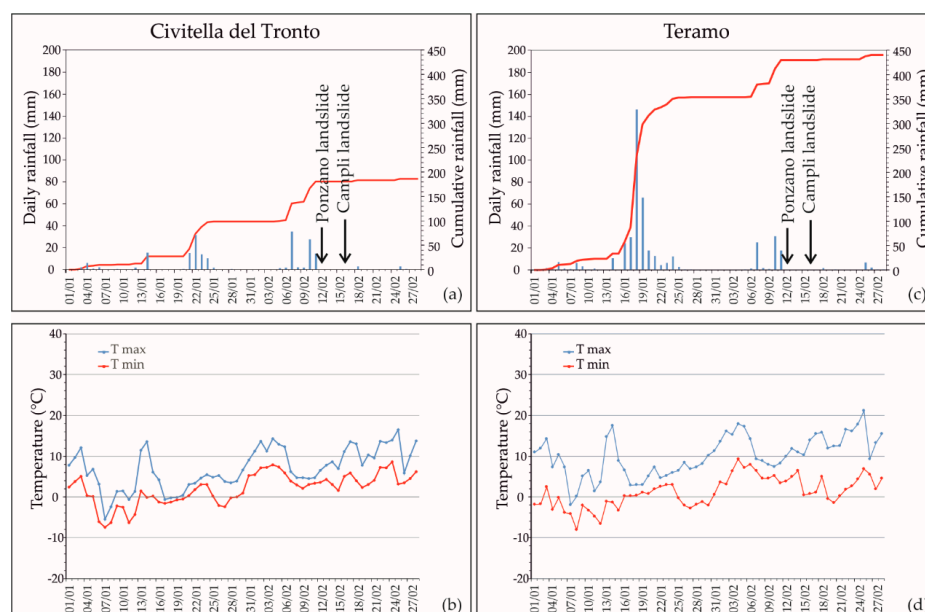


**Figure 3.** Daily rainfall–temperature diagrams for Civitella del Tronto (a,b) and Teramo (c,d) meteorological stations (location in Figure 2).

This induced major damage, civil protection issues (road blockage, large blackout, telephone line failures, aqueduct failures, etc.) and even casualties [17,18]. Temperature and rainfall data for January and February 2017 (provided by the Functional Centre and Hydrographic Office of the Abruzzo Region) were analysed for the meteorological stations of Civitella del Tronto and Teramo, close to the study areas (Figure 2). In both stations (Figure 3), daily rainfall of ~30 mm was recorded during the days before the landslides. In Teramo station, the maximum daily rainfall exceeded 140 mm (18 January, around one month before the sliding) mostly consisting of snow due to low temperature, with a two-month cumulative value of almost 450 mm. Lower values were recorded in the Civitella del Tronto station, with a two-month cumulative value of ~200 mm and no very high daily values. The temperature trend shows two periods with maximum temperatures  $\leq 0$  °C, corresponding to the main snowfall events (around 7–11 and 16–19 January), when many snow avalanches also occurred. From 29 January and again around 11 February, temperature rises occurred, inducing rapid snowmelt.

### 2.1.3. Seismicity

The Central Italy area has been affected by historical and recent strong seismicity [62–64] connected to the Apennine chain extensional tectonics; moderate seismicity also hits the piedmont area. In recent decades, the area was particularly affected by the 2009 L'Aquila earthquake (Mw 6.3) and by the 2016–2017 Central Italy earthquakes (maximum Mw 6.5) (Figure 4). Between 2016 and 2017, Central Italy was struck by a strong and long-lasting seismic sequence that comprised over 65,800 shocks from 24 August 2016 to 30 April 2017. Four main events occurred: (1) on 24 August 2016, two shocks with Mw 5.3 and 6.0; (2) on 26 October 2016, two shocks with Mw 5.4 and 5.9; (3) on 30 October 2016, the strongest, with Mw 6.5; and (4) on 18 January 2017, four shocks with Mw 5.0–5.5 (INGV, [www.ingv.it](http://www.ingv.it)). The latter events were located at 40–45 km SW from the Ponzano and Campli landslides. Moreover, during the first two weeks of February, several minor shocks were recorded (i.e., 283 shocks of Mw 2–3, 22 shocks of Mw 3–4 and two shocks of Mw  $\geq 4$ , at >50 km from the study area; INGV, [www.ingv.it](http://www.ingv.it)). From 10 to 16 February, in the days before the landslide events, 36 shocks occurred with Mw 2.0–3.1 and depths of 6 to 21 km (INGV, [www.ingv.it](http://www.ingv.it)) and a single stronger shock (Mw 3.6) was recorded on 14 February but >40 km from the landslide areas.

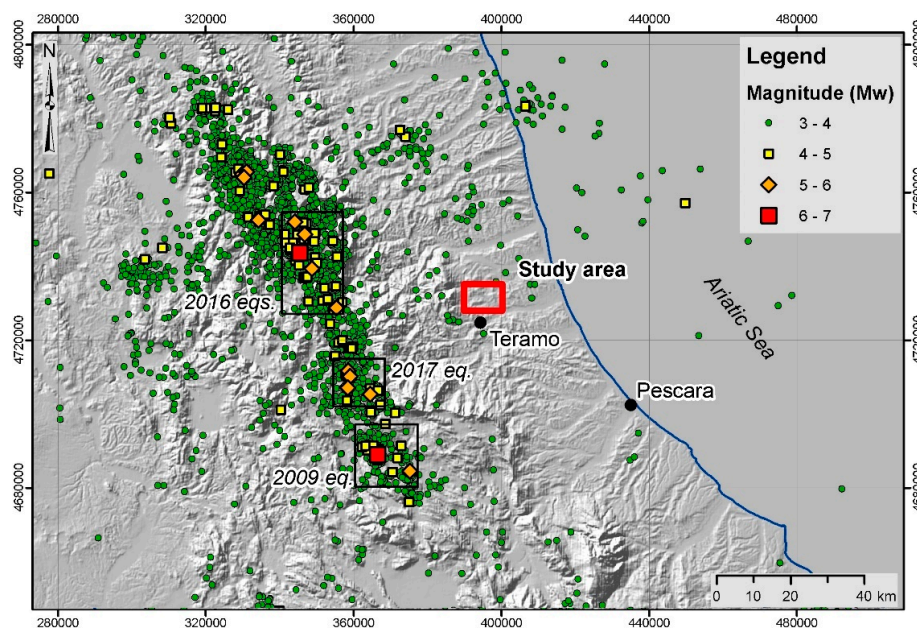


**Figure 4.** Recent seismicity of the Central Italy area and affecting the Apennines piedmont hilly area of NE-Abruzzo; earthquakes (Mw > 4) occurring since 1985 (from ISIDE working group (2016) version 1.0, DOI: 10.13127/ISIDE).

## 2.2. The Ponzano di Civitella del Tronto Landslide and the Castelnuovo di Campli Landslide

The Ponzano landslide (Civitella del Tronto, Teramo) and the Castelnuovo landslide (Campli, Teramo) are located at elevations of 150–400 m a.s.l. in the North-eastern sector of the hilly piedmont of Abruzzo, between the Montagna dei Fiori ridge to the west, the Salinello River valley to the north and the Tordino River valley to the south (Figures 2 and 5). The landscape (typical of the NE-Abruzzo Adriatic hilly piedmont area) is characterized by elongated hills and valleys, generally with a WSW-ENE orientation and secondary from N-S to NNW-SSE orientations. The elevation range is that of mid-to-high elevation hills (from <200 m to >600 m). These hills are crossed by the incisions of the minor watercourses, mostly along NNW-SSE or WSW-ENE orientations. The overall drainage network is arranged in an angular pattern and locally in a trellis pattern.

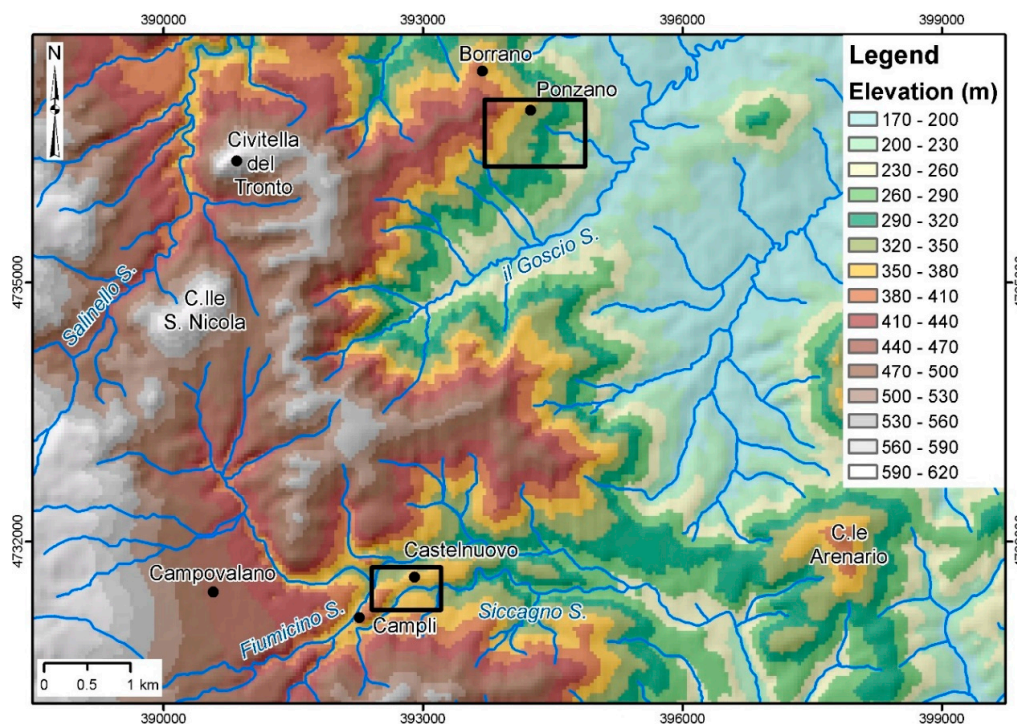


**Figure 5.** Elevation and hydrography map of the study area. The black boxes indicate the Ponzano landslide and Campli landslide areas.

The Ponzano area is located on the Eastern slope of the Civitella-Ponzano WSW-ENE ridge, with a top elevation ranging from 400–550 m a.s.l. Minor sharp NNW-SSE-oriented ridges are present on top of the landslide area. The slope affected by the landslide is around 1.5 km in length and ranges from 400 m to 150 m a.s.l. in elevation with a slope of  $\sim 10^\circ$  (Figure 5). It features flat surfaces in the upper-intermediate area and steep scarps in the upper part as well as in the lower part of the slope. It lies on a NNW-SSE oriented hog-back relief developed on pelitic rocks with thick arenaceous beds (up to tens of meters) pertaining to the Upper Miocene–Lower Pliocene Laga formation. A thick cover of colluvial deposits blankets the bedrock. On 12 February 2017, a large landslide affected Ponzano village, close to Civitella del Tronto (Figure 6a,c,e) reactivating a known landslide [26,58]. The landslide is composed of many connected movements over an area of  $\sim 56$  ha. The overall mechanism was a combination of translational sliding, with local rotational sliding in the upper part, which evolved to flow in the lower part of the landslide. After several years of almost stability or very slow movement (a 10–40 cm deformation was detected in 14 years [22]), the movement developed abruptly in the first days and very slowly over the following months [23]. The landslide involved both agricultural land and inhabited areas. The main and secondary roads, as well as utility service and buildings, suffered serious damage or collapse and consequently, more than 30 buildings were evacuated.

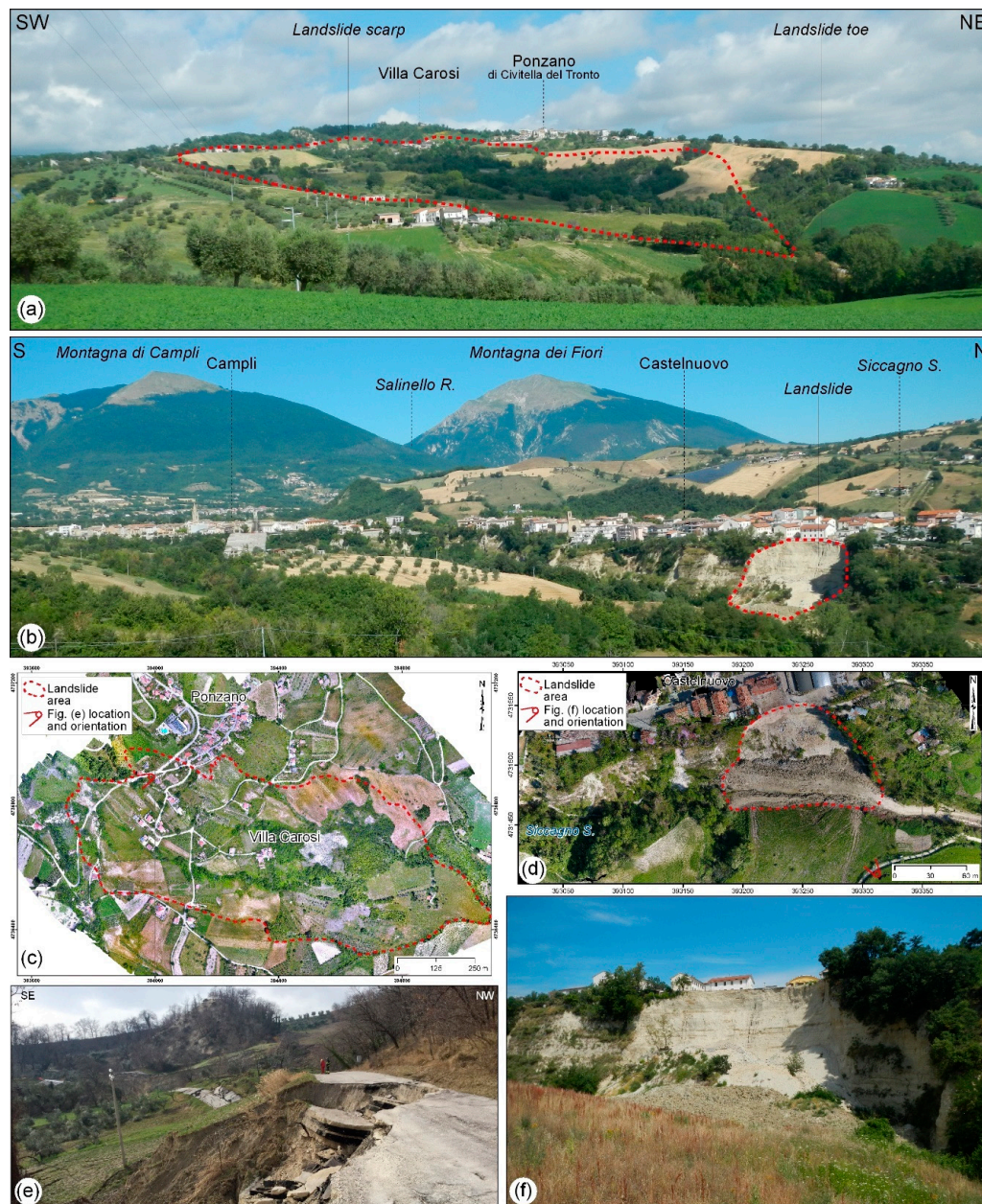


**Figure 6.** (a) Panoramic view of the Ponzano di Civitella del Tronto area (the red dashed line marks the landslide). (b) Panoramic view of the Castelnuovo di Campli area (the red dashed line marks the landslide). (c) Orthophoto of the Ponzano landslide derived by unmanned aerial vehicle (UAV) survey. (d) Orthophoto of the Castelnuovo landslide derived by UAV survey. (e) Panoramic view of the Ponzano landslide scarp. (f) Panoramic view of the Castelnuovo landslide.

The Castelnuovo area is located in the Eastern part of the flat surface hosting the Campli village and is surrounded by steep scarps along the Fiumicino and Siccagno streams. The flat surface ranges in elevation from 350 to 400 m a.s.l., the valleys have elevations of 330 to <300 m a.s.l. (Figure 5) and the scarps are 50–80 m in height and range from very steep ( $>40^\circ$ ) to almost vertical ( $>80^\circ$ ). The landslide area is in the Southern scarp of the flat relief close to a gentle turn of the Siccagno stream. The scarp is very steep with vertical step and drops from ~375 m a.s.l. down to ~315 m a.s.l. The area is characterized by an E-W elongated mesa tabular relief on Middle Pleistocene alluvial fan deposits, incised and terraced during the Upper Pleistocene and Holocene. The deposits consist of moderately cemented conglomerate and sandstone alternated levels and lenses, lying above a marine Pliocene

pelitic-arenaceous bedrock. The mesa relief is rimmed by a structural scarp on conglomerate deposits and its arrangement is controlled by two main systems of joints with WNW-ESE and WSW-ENE orientations. The scarp, particularly in its southern steeper side, is affected by landslides due to fall and topple, complex landslides and weathering producing talus slopes and colluvial deposits at the base. On 16 February 2017, a large collapse abruptly occurred on the southern side of Castelnuovo hill (Figure 6b,d,f). The main landslide affected a semi-circular scarp 100 m in length and ~60 m in height, involving the entire slope from Castelnuovo to the Siccagno stream, which was temporarily dammed by the landslide. The event caused damage such as the collapse of an electric facility and a small house and many houses next to the scarp were evacuated. To the west of the main movement, other minor debris falls occurred during the main event in the following days.

### 3. Materials and Methods

A detailed integrated analysis was performed on the Ponzano and Castelnuovo areas, based on the combination of topographic investigations, by means of an unmanned aerial vehicle (UAV), field geological and geomorphological mapping (1:2000 scale), borehole interpretation, geostructural analysis and photogeological investigation, supported by 3D numerical stability analysis.

The UAV topographic investigation was carried out specifically for this work in order to obtain a detailed post-landslide orthophoto and topographic model of the landslide areas by means of structure from motion (SfM) processing. The images were taken from a DJI Phantom 4 Pro quadcopter (equipped with a 20 Mpx camera) and were processed with Pix4D Mapper. For Ponzano, the images were taken on 1–10 May 2017, with a ground resolution of 10 cm (DSM and orthophoto) and 1 m derived contour lines; for Castelnuovo, the images were taken on 14 April 2017, with a ground resolution of 3.5 cm (DSM and orthophoto) and 1 m derived contour lines. Together with pre-landslide aerial photos and DEMs, the UAV aerial photo also supported the geomorphological and displacement analysis of the landslide.

The field geological and geomorphological mapping, with geostructural analysis, was carried out after the landslides' occurrence at 1:1000 scale according to the guidelines of the Geological Survey of Italy (ISPRA). It was focused on the definition of: (1) the bedrock units and superficial deposits involved; (2) the geometry and distribution of joints affecting the rock masses; and (3) the main geomorphological features developed during the sliding (e.g., major and minor scarps, cracks, landslide terraces, counterslopes, landslide features, etc.). The field survey was supported by the analysis and interpretation of borehole data (derived from previous studies for the seismic microzonation of the Campi area [64]) in order to constrain the thickness of the lithological units. The main geotechnical parameters were also derived from previous microzonation studies [64].

For the Ponzano landslide, a detailed air-photo interpretation was carried out comparing pre-landslide orthophotos (Flight Abruzzo Region, 2007 and 2010) and post-landslide UAV orthophotos [65]. UAV imaging is largely used as a tool for detailed post-landslide monitoring [66,67] as already done in the Ponzano landslide for a fine post-event displacement analysis [23]. In our work, however, the UAV images were compared with the available pre-landslide aerial photos (taken on 2010 and 2013, source <http://geoportale.regione.abruzzo.it/Cartanet>). From 2010 and 2013, before the 2017 landslide, no or very slow (<40 cm in 14 years.) movements were detected in the area [22,23], making this comparison suitable to provide an overall displacement analysis of the landslide. Around 240 homologous points (building, roads and other structures) were defined for the comparison (avoiding the uncertain ones). The resolution of the analysis is coarse (~±1 m) and, for this reason, the movement of each point was tracked considering only values above 2 m. Nevertheless, the points' comparison allowed defining the distribution of the overall deformation occurred on the slope from the landslide event to May 2017 and the displacement pattern of the landslide. A more detailed post-landslide integrated monitoring is provided in Allasia et al. [23].

For the Castelnuovo landslide, a 3D numerical modelling (FLAC3D, Itasca [68]) was carried out, through several specific pre- and post-landslide stability analyses. The post-landslide 3D geometrical

reconstruction of the slope was based on the UAV-derived contour lines. For the pre-landslide slope, the UAV-derived contour lines were integrated, in the landslide area, with contour lines derived from the 2007 1:5000 scale topographic map and interpolated from aerial photos (Flight Abruzzo Region, 2007) provided by the Abruzzo Region Cartographic office (<http://opendata.regione.abruzzo.it/>). According to the results of the geological, geomorphological and geostructural investigations, as well as borehole data, a 3D model of the slope was defined and summarized in three geomorphological cross-sections. The main joints, whose geometry was derived from the field survey and remote investigations, were incorporated in the model defining a set of conglomerate-sandstone polygonal wedges. The analysis was performed in the pre-landslide condition, taking into account both dynamical seismic shaking and pore water pressure, in order to investigate the triggering of the landslide and the connection with previous seismic shaking and snowfall–rainfall events. The post-landslide analysis was performed specifically to investigate the current stability conditions, both in the landslide area and in the surrounding scarp, to investigate the residual stability conditions. In order to understand the contribution of the different factors (lithology and joints, seismic shaking, pore pressure), the stability analysis of both models (pre- and post-landslide) was carried out for the following scenarios: (A) simple model with no joints; (B) complete model with joints; (C) dynamic analysis of the complete model with joints; (D) pore water pressure analysis on the simple model.

Scenarios A and B supported the analysis of the control of lithology and jointing in the stability and failure kinematics. In order to investigate the critical areas and the failure kinematics, the stability analyses were carried out progressively reducing the strength parameters taking the slope to the failure conditions. Scenario C was focused on the analysis of seismic shaking as a triggering factor of the landslides, choosing one significant input from the 2016–2017 seismic sequence of Central Italy (Figures 2 and 4)—specifically, the closest event (i.e., 40–45 km) with a  $M_w \geq 5$  to the landslide area, that is, the 18 January 2017 event (time 11:14:09), which had a  $M_w$  of 5.5 and epicentre in the Capitignano (L’Aquila) area. The accelerogram was acquired from the ITACA Database (the INGV accelerometric archive [69]) for the Terelle accelerometric station (Table 1). The station was selected since it is the closest to the Campli area (located ~12 km south of the landslide site) and the only one that lies on soil class “A” in the surrounding area (Table 1). The input accelerograms, in the N-S and E-W components (properly scaled according to Bindi et al. [70]), were applied at the base of the model respectively in the y and x direction. Scenario D allowed the role of pore water pressures in the stability conditions and in the landslide triggering to be evaluated. In order to simulate the increasing pore pressures related to the extreme meteorological events (snow, rainfall) preceding the landslide, as well as the leaching from urban water pipes, the top 15 m of the model (from the top of the scarp) were supposed to be saturated.

**Table 1.** Details of the Terelle Accelerometric Station from the ITACA Database (the INGV accelerometric archive [69]).

Station Code	TER
City, Region	Teramo, Abruzzo
Latitude [WGS84]	42.65656
Longitude [WGS84]	13.68954
Soil class (EuroCode8)	A
Topography category	T1—Flat surface, isolated slopes and cliffs with average slope angle $i \leq 15^\circ$

## 4. Results

### 4.1. The Ponzano di Civitella del Tronto Landslide

The Ponzano landslide is a large (1.4 km in length, 0.6 km in width, 56 ha surface area) composite landslide with multiple complex movements related to mechanism from translational sliding with local rotational components, in the upper part, to translational sliding/flow in the lower part. The recent

movement occurred abruptly on 12 February 2017 and slowly in the next few days, as reactivation of previous large landslides that affected the slope.

#### 4.1.1. Geological Model and Morphostructural Setting

In the Ponzano area, the bedrock consists mostly of a sequence of pelitic-arenaceous layers (Figures 7 and 8). The ridges to the west of Ponzano consist of 30–60-m-thick layers of sandstone with thin clay levels (Figure 7).

The layers are arranged in a NNW–SSE orientation, dip at 40–60° in an ENE direction and are locally folded. The bedrock is blanketed by a cover of colluvial deposits (up to 15 m in thickness) and landslide deposits (up to 70 m in thickness). The morphostructural setting consists of a NNW–SSE oriented double hog-back (Figure 8). The landslide involved the whole colluvial cover and the upper part of the clayey bedrock (Figure 9).

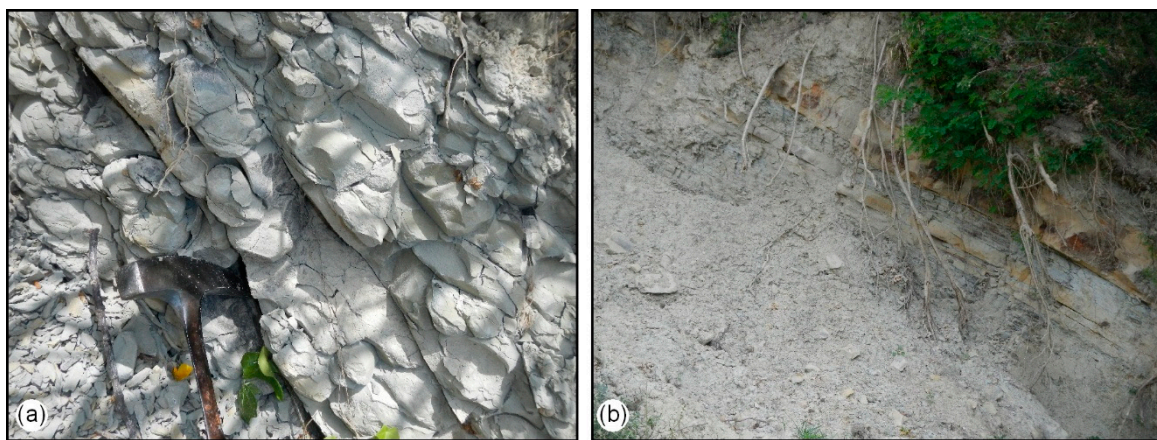


**Figure 7.** Lithological features of the bedrock arenaceous layers in the Ponzano area: (a) thick sandstone layers; (b) alternating sandstone layers with thin clay levels.

#### 4.1.2. Geomorphological Features

In the upper part of the slope, two paired sharp ridges outline a NNW–SSE oriented hog-back connected to the steep ENE-plunging sandstone layers interbedded in the pelitic sequence. These ridges control the setup and shape of the main landslide scarps. They are arranged in a double arcuate scarp system. The southern system is composed of at least two-to-three main scarps up to 350–400 m in width and from 2 m to >10 m in height and outline local counterslopes and rotational sliding (Figure 10a). The Northern one is a secondary arcuate scarp system (closely affecting Ponzano village). It is composed of a system of scarps up to 150 m in width and from a few decimetres to 10 m in height (Figure 10b). Upslope from the main scarp systems sets of minor scarps and tension cracks are present and outline the regressive trend of the landslide. The middle part of the landslide is composed of many combined sliding blocks separated by secondary scarp and characterized by counter slopes, ridges and bulges. The southern lateral scarp of the landslide (Figure 10c) is undulated and characterized by scarps up to 2 m in height (Figure 10d). On the scarps, strike-slip ENE-dipping grooves outline a clear translational component of the landslides (Figure 10d) and, along the scarp, local push ridges are present (Figure 5f).

The centre of the landslide is characterized by counter slopes, ridge or bulging, which outline a large landslide terrace in the mid-to-upper part of the slope, largely affected by tension cracks and minor scarps (Figure 10f). This area was the most severely damaged, with several buildings being destroyed due to a large bulging. During the sliding, this area was pervasively affected by tension cracks, trenches and occasionally by pseudo mud volcanoes connected to mud ejection. The northern side of the landslide is a system of minor sliding blocks mostly connected to translational sliding. The mid-to-lower part of the slopes was affected by several minor scarps (both downslope and

upslope (Figure 10g), push ridges and bulging outlining the complex movement of the landslide with translational sliding combined with flow. The mid and lower parts of the landslide are affected by minor gully features, which affected the area before and after the 2017 sliding.

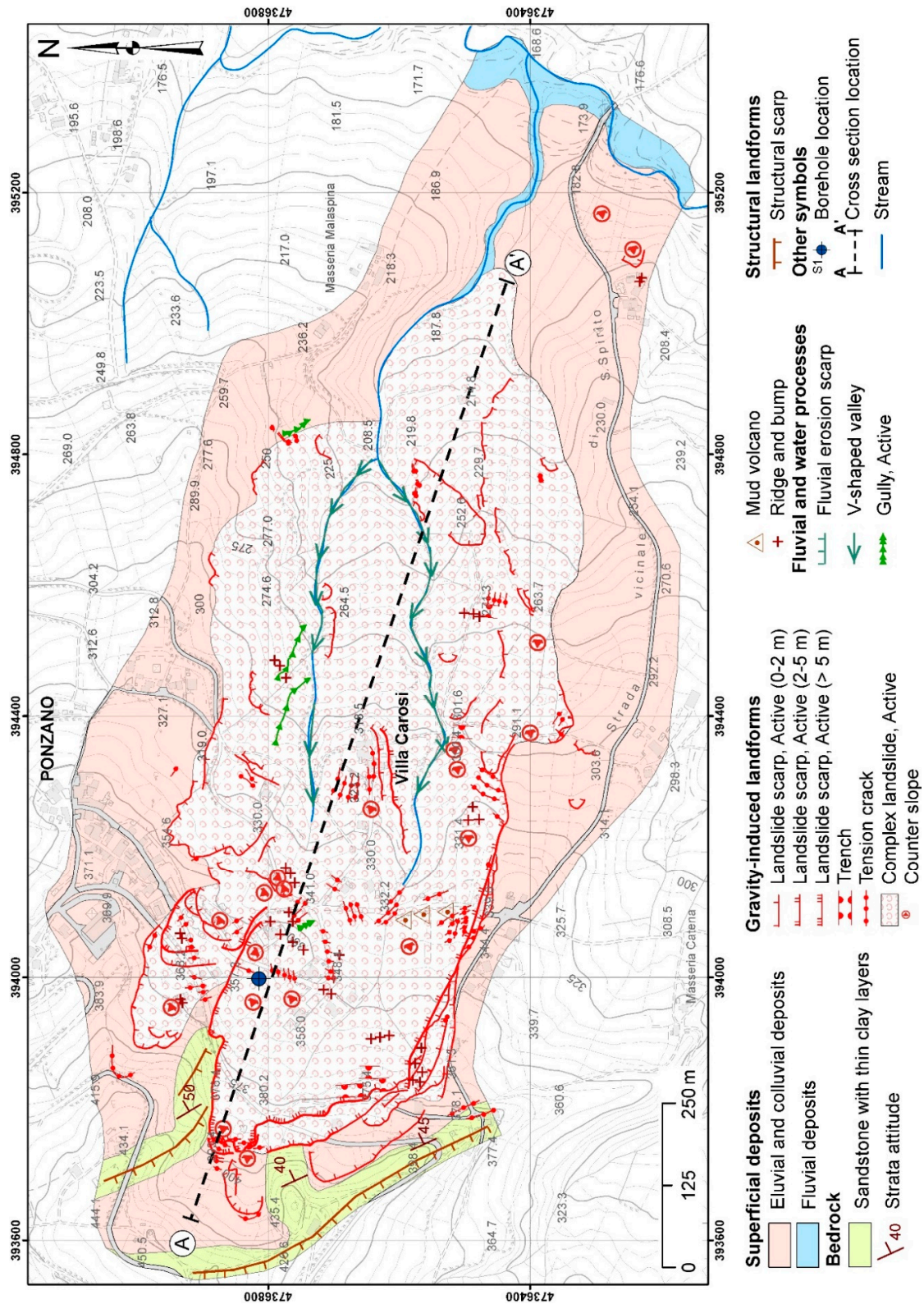
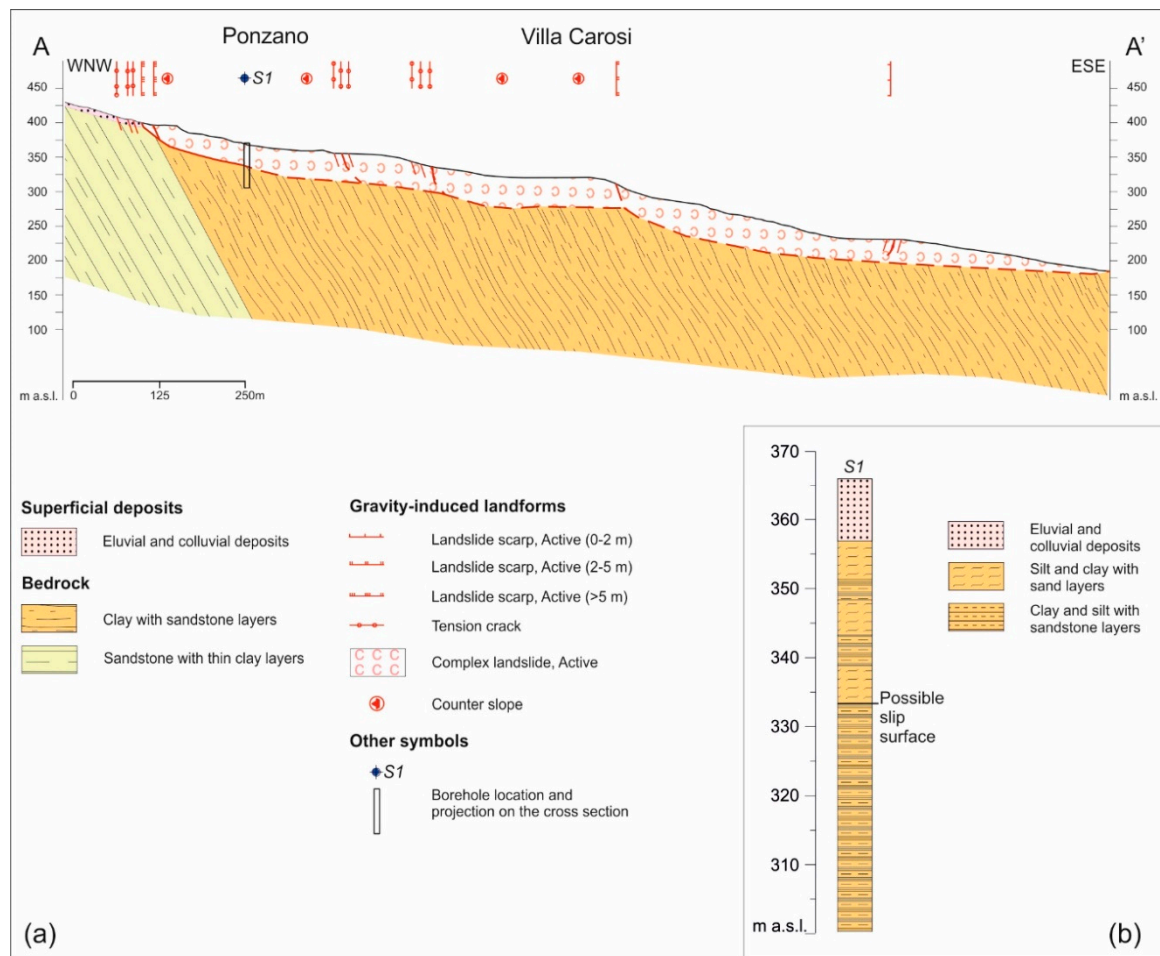


Figure 8. Geological and geomorphological map of the Ponzano area.



**Figure 9.** (a) Geological and geomorphological cross-section of the Ponzano area (location in Figure 8). (b) Stratigraphy of the borehole S1 (location in Figure 8).

### 4.1.3. Displacement Pattern

A photogeological analysis of pre-landslide (2010–2013 orthophoto) and post-landslide (May 2017 UAV survey) orthoimages of the Ponzano landslide area was carried out in order to investigate the displacement pattern of the landslide and to outline the different blocks of the composite landslide (Figure 11a). The displacement of ~240 homologous point in pre and post-landslide images (e.g., roads, houses, etc., Figure 11b–f), although with a poor resolution (~±1 m), outlined a displacement varying within the landslide from almost zero to >18 m toward ESE. The analysis outlined the highest deformation (up to >15 m) to have occurred in three main areas within the landslide. One located in the upper part close to the main Southern scarp; the second in the central part along the landslide terrace (south from Ponzano); and the third one in the mid-to-lower part, downslope from Villa Carosi. The displacement is up to 13 m along the southern lateral scarp of the landslide, while it decreases to zero in the northern scarp and in the northern side. Downslope, the displacement decreases and progressively drops to zero in the lower part of the landslide.



**Figure 10.** Geomorphological features of the Ponzano landslide. (a) upper part of the main southern scarp (up to >10 m high); (b) main northern upper scarp close to the Ponzano village (up to 5 m high); (c) lateral scarp in the southern side of the landslide; (d) detail of the lateral scarp, with grooves outlining the translational movement; (e) push ridges on the southern lateral scarp; (f) tension cracks in the mid part of the landslide; (g) minor scarps in the mid-lower part of the landslide.

The deformation is documented to have occurred mostly on 12 February 2017 and in the next few days (up to >8 were detected by a GPS survey carried out by the Civitella del Tronto Municipality [23], after a pre-2017 very slow movement [22]), which is congruent with our geomorphological field observation. Moreover, after 23 February and in the following months, a detailed monitoring of the landslide documented minor and localized movements connected to the main rainfall events (5–65 cm in ~5 months [23]).

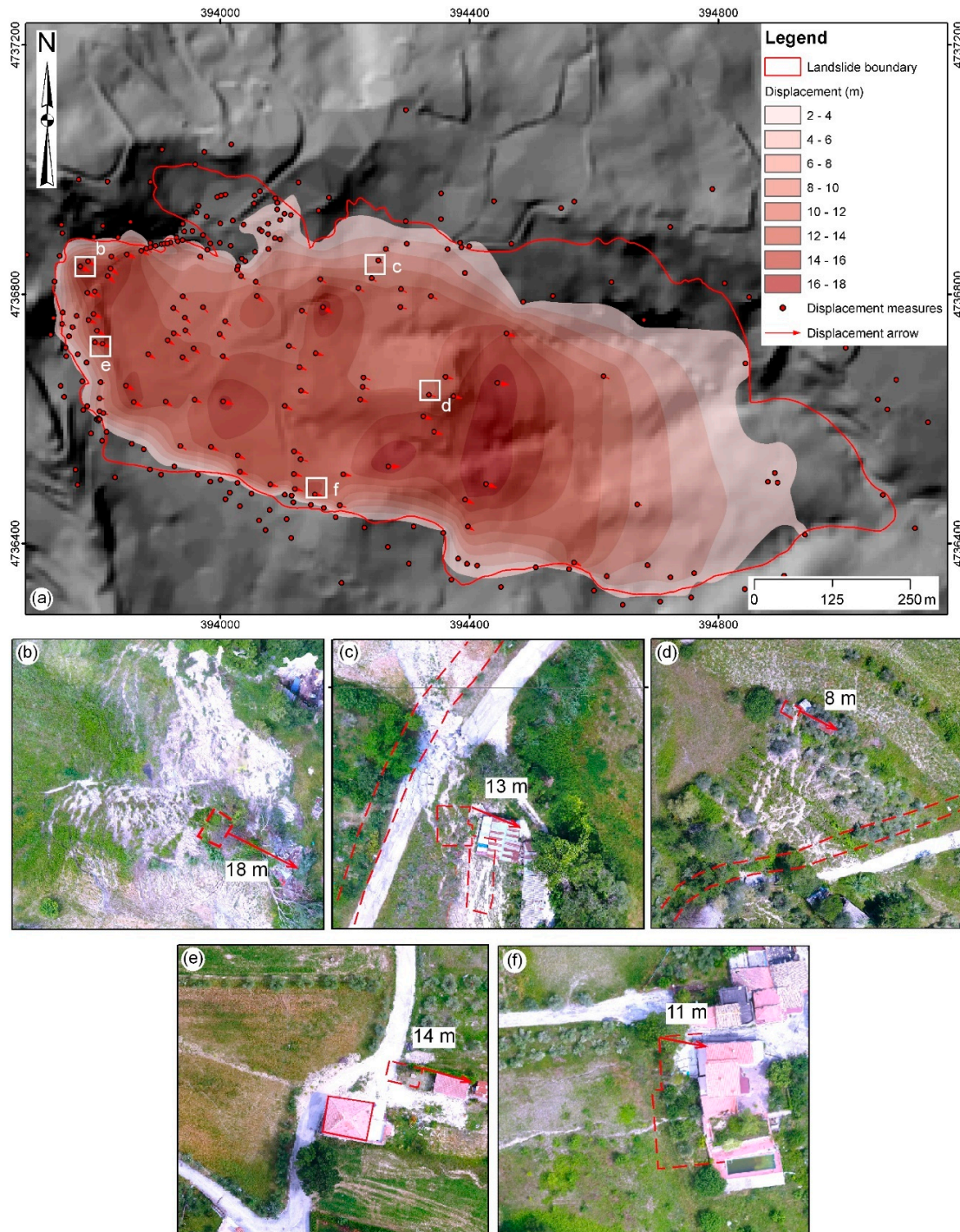


**Figure 11.** (a) Displacement distribution in the Ponzano landslide. (b–f) Significant measurement points observed in the landslide area; the image is derived from UAV post-landslide orthophoto and the red dashed lines mark the pre-landslide locations (derived from 2010 orthophotos); the measurement location is in (a).

#### 4.2. The Castelnuovo di Campli Landslide

The Castelnuovo landslide is a complex landslide induced by a collapse affecting the moderately cemented conglomerate and sandstone along the southern side of the Campli-Castelnuovo mesa relief. Additionally, in this case, the combination of topple/fall and slide movements was controlled by the morphostructural features of the mesa relief consisting of two systems of main joints (WSW-ENE and WNW-ESE oriented). The landslide affected a 100 m-wide sector of the structure-controlled scarp bounding the mesa relief for its entire height from ~375 m to ~315 m a.s.l. and down to the Siccagno stream for a length of ~80 m (total area ~0.8 ha). It occurred suddenly and very fast in the night of 16 February 2017 and affected several human-made structures, such as minor buildings and facilities of Castelnuovo village. Some main houses next to the landslide scarp were suddenly evacuated and demolished in the following months.

##### 4.2.1. Geological Model and Morphostructural Setting

The geological model of the Castelnuovo area consists of a thick conglomerate-sandstone interval, arranged in decimetre-to-meter-thick conglomerate layers, with minor sand-sandstone layers and lenses and with weak to moderate cementation (Figure 12). The whole conglomerate-sandstone interval is up to 70 m in thickness and lies above pelitic-arenaceous rocks of the bedrock, as documented in previous borehole investigations, with the bottom of the layer lying below the base of the scarp (Figure 13). The conglomerate-sandstone layer thickness decreases toward the south and north and outlines that the alluvial fan deposits filled up a paleo valley, whose axis is now below Castelnuovo village.

The morphostructural setting is characterized by a well-defined mesa relief. The geostructural analysis defined two systems of large joints (several tens of meters in length) affecting the conglomerate rocks of the mesa relief (Figure 14). The main system is oriented WNW–ESE and is mostly vertical or dipping at 60–70° to the NE. A secondary system is oriented ENE–WSW and dips at 70–80° to the NW to the SE. These systems observed at the local scale are parallel to the orientation of the main and secondary scarps affecting the Castelnuovo relief and the relief top. More generally, these orientations are consistent with the main orientations of the geomorphological evidence of tectonics documented in the entire Northern Abruzzo piedmont area [51], which confirm that the joints observed in the Castelnuovo area are not local features but rather related to major features.



**Figure 12.** Lithological features of the terraced Middle Pleistocene alluvial fan deposits: (a) alternating gravel (g), sand (s) and clayey-sand (s-c) on the entire landslide scarp; (b) close up of the lithological features of the scarp.

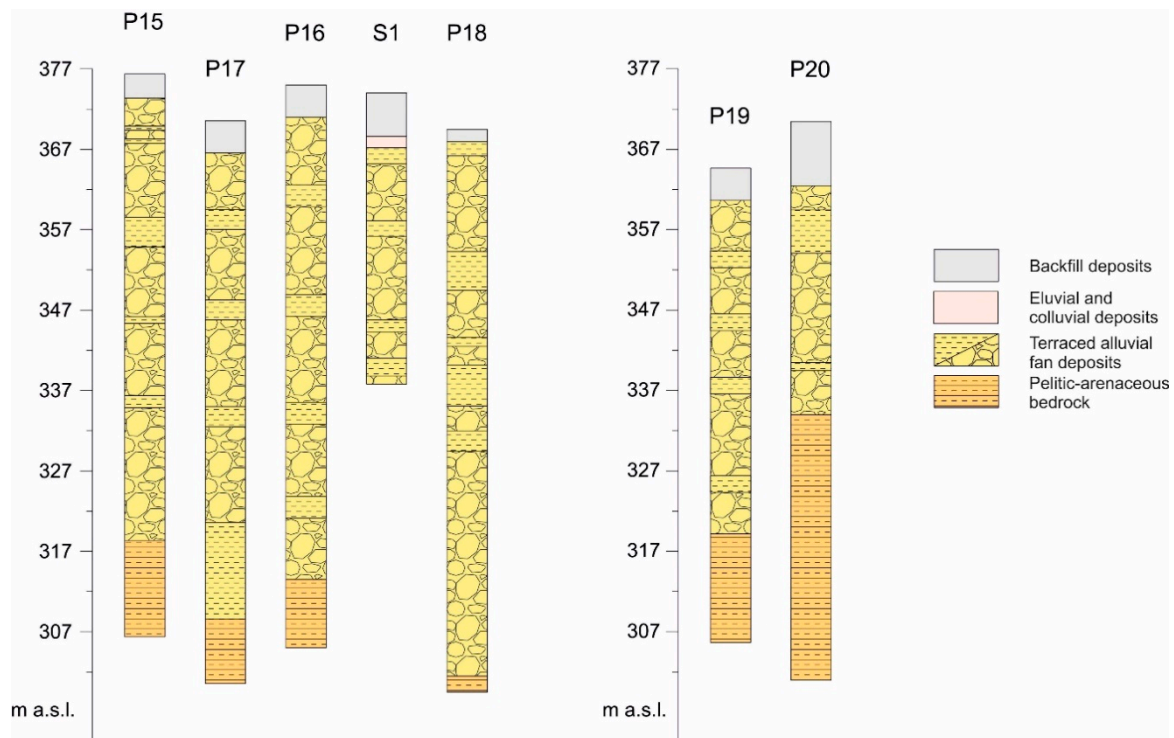


**Figure 13.** Borehole stratigraphy of the Castelnuovo area (location in Figure 14).

#### 4.2.2. Geomorphological Features

The landslide scarp has an easily visible and homogeneous semi-circular shape and a height of several tens of meters (Figure 15a,b). The landslide body fell down into the Siccagno valley and climbed up the opposite side of the valley partially obstructing the valley itself. The entire southern Castelnuovo slope features talus slopes and minor landslides. Some are old and dormant, while others (falls and slides) occurred in February 2017 and in the following months. The minor landslides have variable size (from 15 to 25 m in length and 10 to 30 m in width). After the landslide, the main accumulation was partly removed and reworked in order to restore the Siccagno drainage (Figure 15c). In the last year, remediation works have been implemented in order to stabilize the landslide scarp and the base of the scarp, although they involved the scarp partially and are still in progress. The southern side of the Siccagno valley features the toe of a large dormant complex landslide. It was partly reactivated by a minor landslide due to flow after the Castelnuovo landslide.

In addition to the main gravity-induced landforms, structural landforms, landforms induced by surface running waters and anthropogenic landforms are present. The structural landforms are mostly related to the mesa relief and to its main scarps (Figure 15c). They are polygenetic landforms, which originated as fluvial terrace scarps during the incision of the Fiumicino and Siccagno streams. They were then preserved due to the structural control of consistent conglomerate and sandstone rocks and were recently largely affected by landslides.

Minor (1–3 m in height) scarps are also present breaking the top surface of the mesa relief. The arrangement of both minor and major scarps is strictly connected to the orientation and location of the main joints affecting the conglomerate rocks. This arrangement outlines major and minor structural surfaces and benches at the top of the mesa relief (Figure 15d). The minor ones are present mostly in the southern part of the mesa relief and the base of the scarps is partially filled by colluvial wedges.

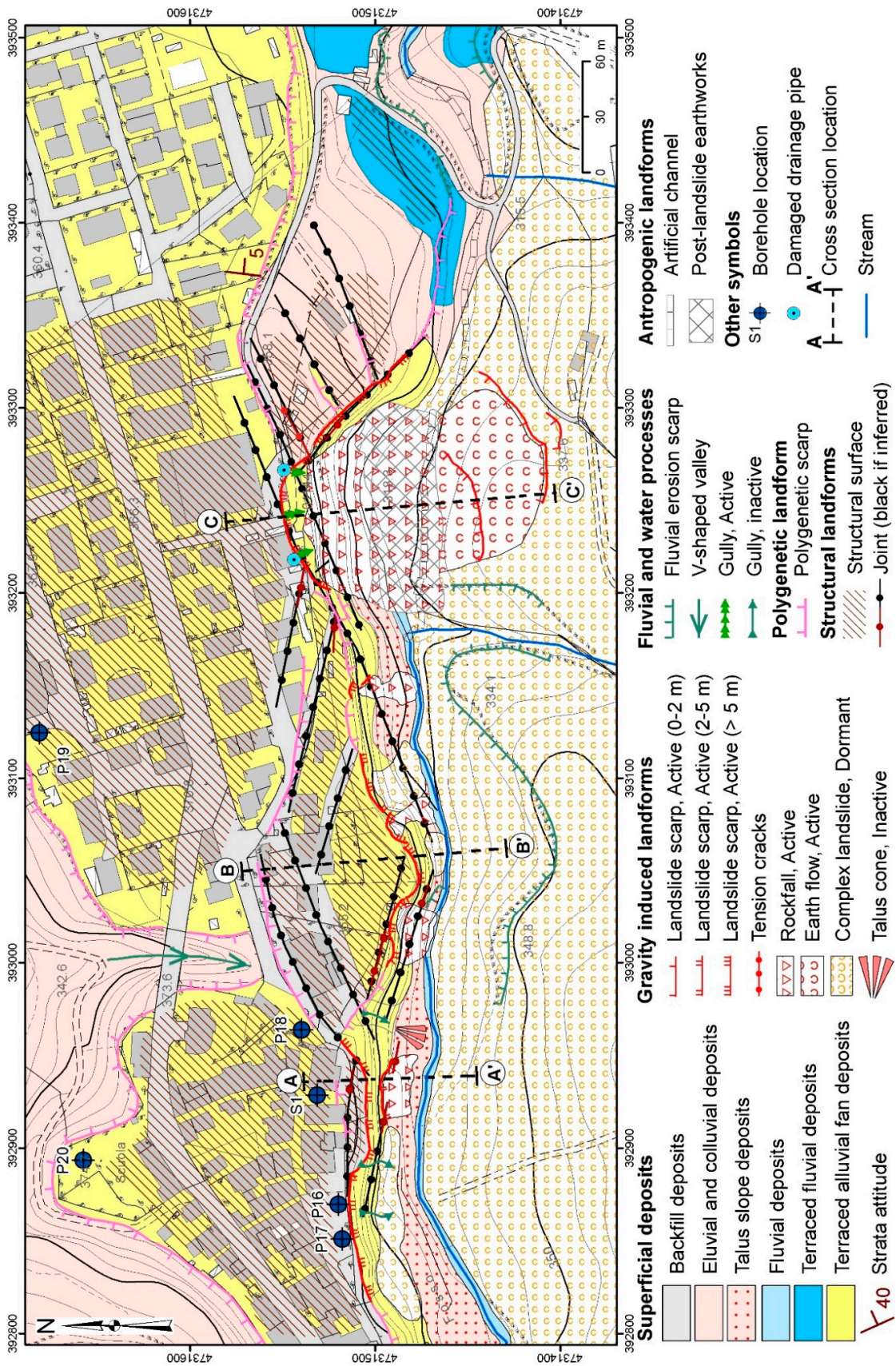


Figure 14. Geological and geomorphological map of the Castelnuovo area.



**Figure 15.** Geomorphological features of the Castelnuovo landslide: (a) main landslide scarp (western part); (b) main landslide scarp (eastern part); (c) polygenetic scarps (red arrows) of the Castelnuovo mesa relief (in the foreground the landslide body); (d) structural surface (red arrows) on top of the main scarp; (e) fluvial erosion scarp at the base of the main scarp; (f) damaged water pipe along the landslide scarp; (g) tension crack along a joint affecting the slope; (h) main joints affecting the slope in the landslide area.

Minor fluvial and water erosion landforms are V-shaped valleys and gullies, which affect the scarp and outline the present water drainage; fluvial erosion scarps affect the base of the main scarp (Figure 15e) and incise the southern side of the Siccagno valley. Furthermore, in addition to the largely reworked top surface of the Castelnuovo relief, which is outlined by the extensive accumulation of backfill deposits (only those >2 m in thickness are mapped in Figure 14), the main earthworks and artificial channel are mapped, related to the post-landslide remediation works.

Damaged drainage pipes are also to be mentioned. Two of them were found in the main scarp area (Figure 15f) inducing possible water drainage issue and additional infiltration in the scarp area during the heavy meteorological events and the snowmelt.

The overall setting of the main scarp are defined by combined features outlining a polygenetic scarp surrounding the mesa relief: (1) a step-like arrangement to the top surface given by minor straight 1–5 m-high scarps, oriented from WNW–ESE to ENE–WSW; (2) an angular arrangement of the main scarp bounding the top surface along the same WNW–ESE and ENE–WSW orientations, consistent with the orientation of the main joints (Figure 15g,h).

The main geological and geomorphological features outline the 3D geological and morphostructural model of the Southern slope of the Castelnuovo mesa relief (Figures 14 and 16). It is characterized by polygonal conglomerate-sandstone wedges (as large as 20–50 m in width, 80–120 m in length and ~50–70 m in height) separated by major joints, laying over the pelitic-arenaceous bedrock. The investigation allowed also to define the pre-landslide geological and morphostructural model summarized in the section of Figure 17.

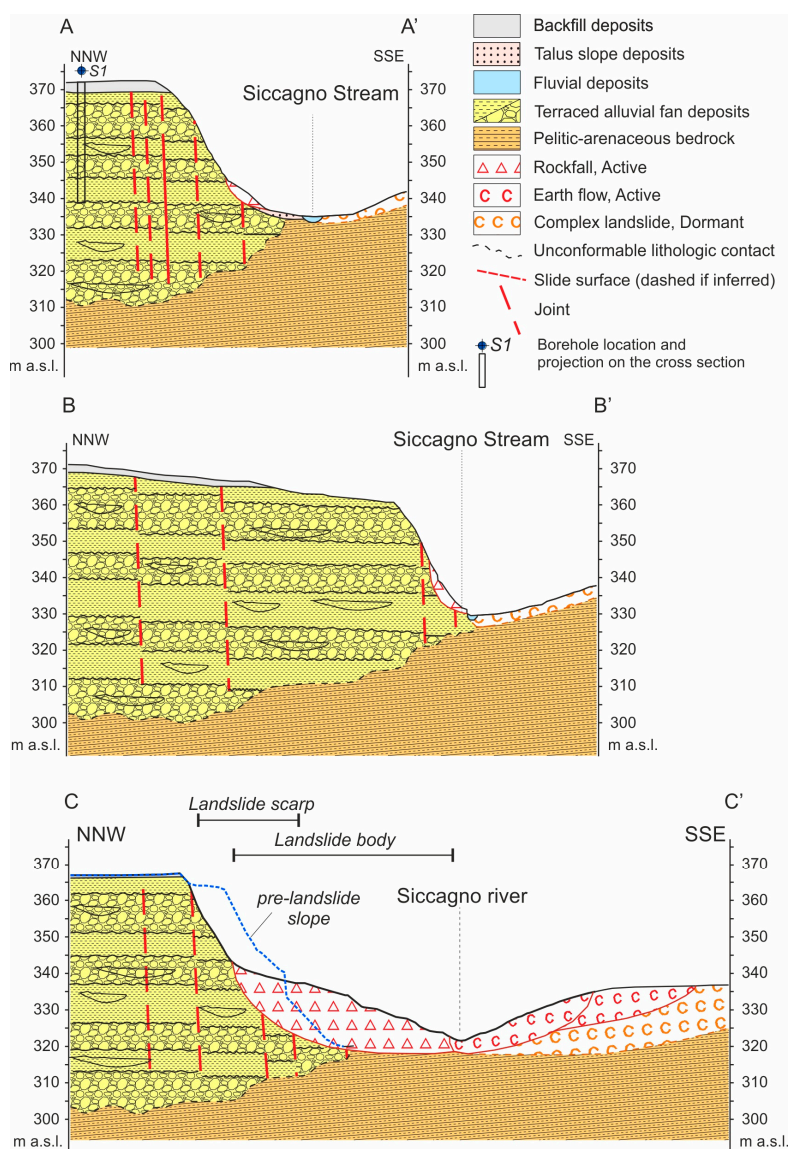


**Figure 16.** Geological and geomorphological cross-sections of the Southern slope of the Castelnuovo area (location in Figure 14); in Section C-C' the dashed blue line show the reconstructed pre-landslide topography (cfr. Figure 17).

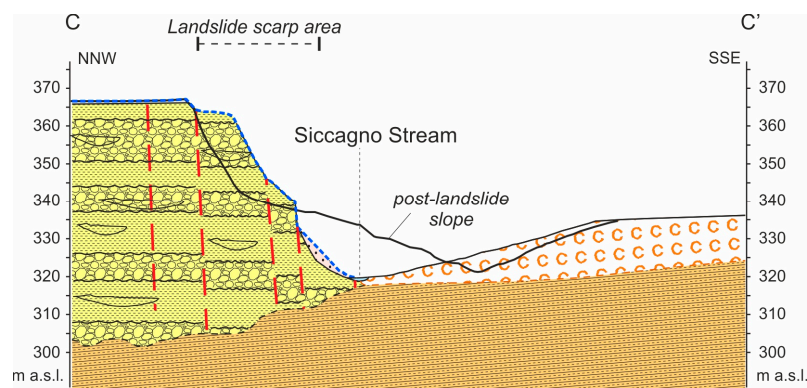


**Figure 17.** Pre-landslide geological and geomorphological cross-sections of the Castelnuovo landslide area (location in Figure 14); the thick black line is the post landslide topography (cfr. Figure 16).

#### 4.2.3. Landslide 3D Modelling

Two 3D models were defined for the numerical modelling: the first in the pre-landslide conditions in order to investigate the trigger of the 16 February landslide and the second in the post-landslide conditions to investigate the expected evolution of the landslide and the residual hazard condition. Both models are 544 m in length ( $x$ -axis), 188 m in width ( $y$ -axis) and 84 m in height ( $z$ -axis) discretized with variable-sized tetrahedral elements. The models consist of conglomerate-sandstone wedges, while the bedrock is not included since it lies over 15 m below the base of the slope along the Siccagno stream (Figure 16). The main physical-mechanical parameters (assumed constant throughout the model) are [65]: volume weight ( $21 \text{ kN/m}^3$ ), bulk modulus ( $66.7 \text{ MPa}$ ), shear modulus ( $40 \text{ MPa}$ ), internal angle of friction ( $35^\circ$ ) and apparent cohesion ( $30 \text{ kPa}$ ).

Dynamic numerical analysis was also carried out using dynamic modules such as stiffness parameters calculated by the mean of the S- and P-wave velocity values obtained from down-hole tests:  $V_s = 500 \text{ m/s}$ ;  $V_p = 2300 \text{ m/s}$ .

##### Pre-Landslide Model without Discontinuities

The first analysis was carried out on a pre-landslide simplified model, not including the main joints, in order to verify the validity and the numerical stability of the model. The analysis of the displacement diagrams (Figure 18) shows two critical areas: one in the western part of the model and the other in the area already affected by the landslide event. In order to better understand the evolution of the entire slope, three significant sections were extracted outlining the kinematic evolution of the entire scarp. They highlight the potential pseudo-circular slip surfaces that develop from the top of the scarp (20–30 m from the edge) down to the foot of the slope.

##### Pre-Landslide Model with Discontinuities

The second analysis was carried out in the complete pre-landslide model with the main discontinuities outlining polygonal wedges. The displacement diagrams (Figure 19) show the control of the joints in the evolution of the slope and in the failure kinematics. The most critical areas, in terms of deformation, are located along the main joints up to 20–40 m from the edge of the scarp, in the area surrounding the main landslide. The sections extracted from the model (Figure 19) help to identify the role of the joints in the failure kinematics. The displacement vectors of the outermost slope part, out of the last joint, range from horizontal to gently downslope dipping, outlining a topple movement. The inner part of the slope shows steep downslope displacement vectors, outlining a pseudo-circular slip kinematics, again controlled by the main joints in the inner part of the slope.

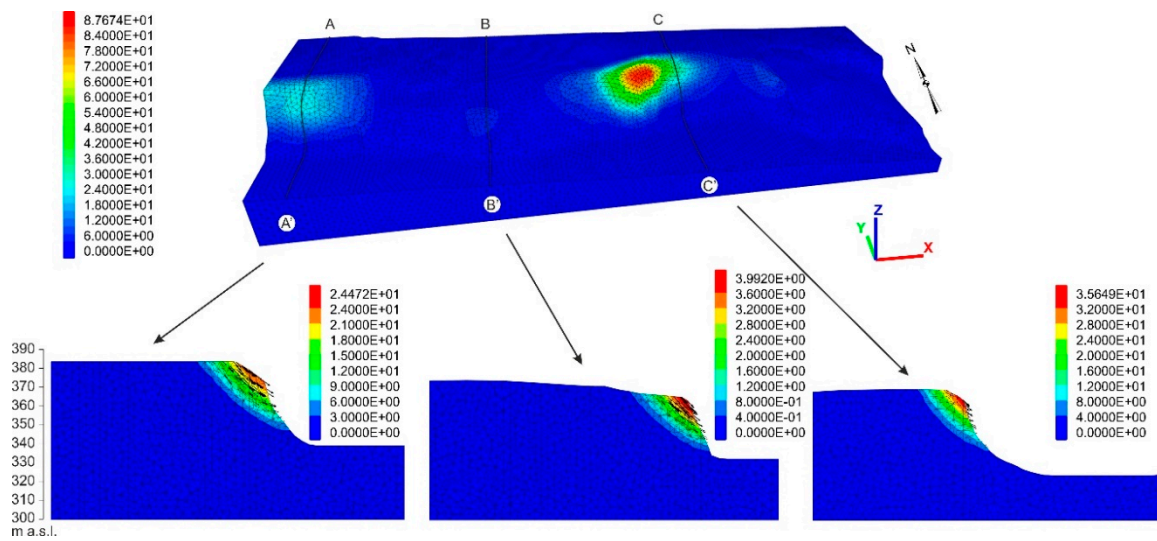


**Figure 18.** Contour 3D displacements and displacement vectors (sections) of the pre-landslide model without discontinuities.

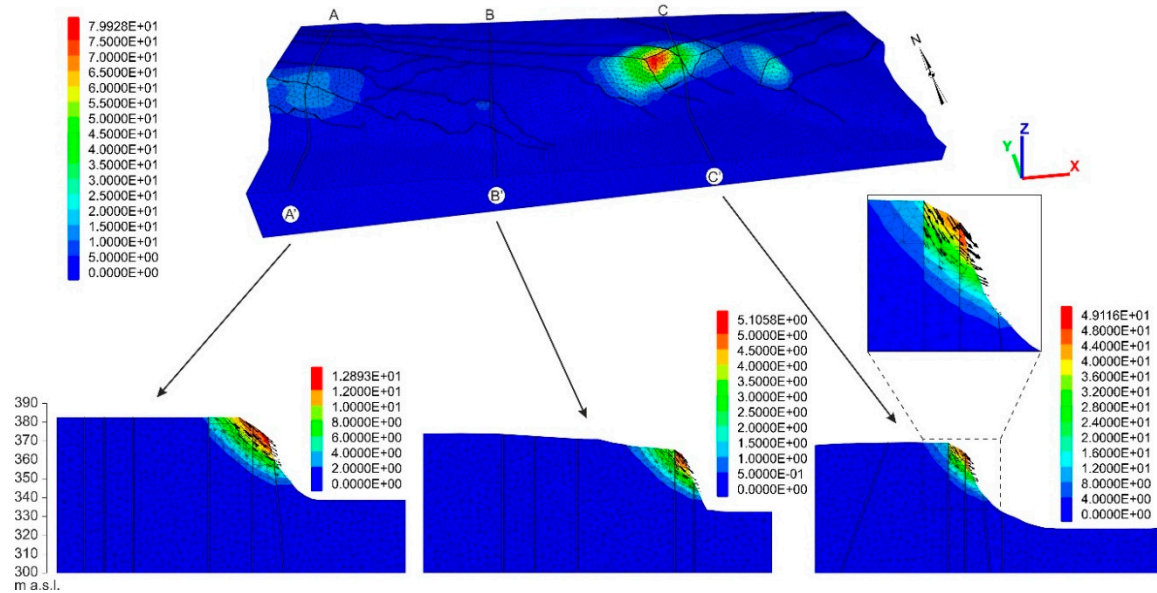


**Figure 19.** Contour displacements and displacement vectors (sections) of the pre-landslide model with discontinuities.

### Pre-Landslide Dynamic Analysis of the Model with Discontinuities

The dynamic analysis was performed on the complete pre-landslide model (with discontinuities) introducing the seismic input chosen among those recorded in the long 2016–2017 seismic sequence of Central Italy (the Mw 5.5 event occurred on 18 January 2017, around one month before the landslide). The largest displacement occurs in three main areas (Figure 20), which correspond to those expected from the field survey. This is particularly evident in the western area and in the Eastern area, which includes the main landslide area. However, even in dynamic conditions, the model does not reach the failure. As documented by the displacement vectors in the extracted sections, in this case, the deformation kinematics are also controlled by the main joints.

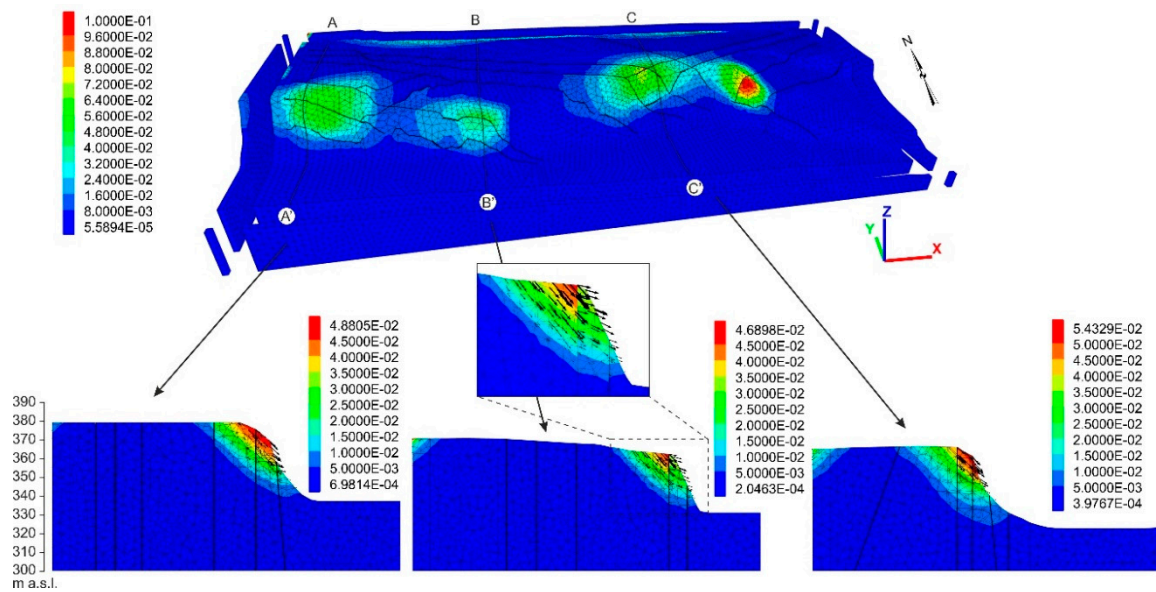


**Figure 20.** Contour displacements and displacement vectors (sections) of the dynamic analysis with Mw 5.5 input on the pre-landslide model with discontinuities.

#### Pre-Landslide Model without Discontinuities and with Pore Water Pressures

The fourth analysis was carried out to evaluate the influence of pore pressures on the slope stability, introducing water saturation in the upper 15 m of the model from the top of the scarp (Figure 21a).

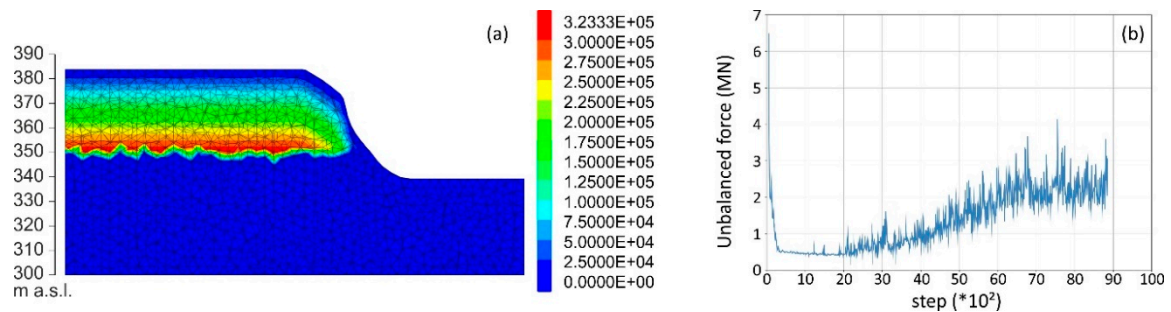


**Figure 21.** (a) Detail of pore pressures in the pre-landslide model. (b) Maximum unbalanced force in the model.

In this case, the slope reaches the failure (Figure 21b), highlighting the non-convergence of the numerical algorithm of the maximum unbalanced force. All of the outermost wedges of the model, along the main scarp, result to be in failure conditions (Figure 22).

#### Post-Landslides Model with Discontinuities

A further set of analyses was carried out in the post-landslide model in order to investigate the residual instability conditions after the main landslide. The stability analysis without or with discontinuities, also in this case, outline no failure (static model and no pore pressure) and again suggest the role of the main joint in the expected kinematics of the deformation. The worst critical area resulting from the model with discontinuities (Figure 23) is located along a main joint in the eastern side of the February 2017 landslide scarp. Again, the extracted sections outline the complex kinematics of the expected movement: a combination of toppling in the outer wedge of the slope and sliding in the inner wedge.

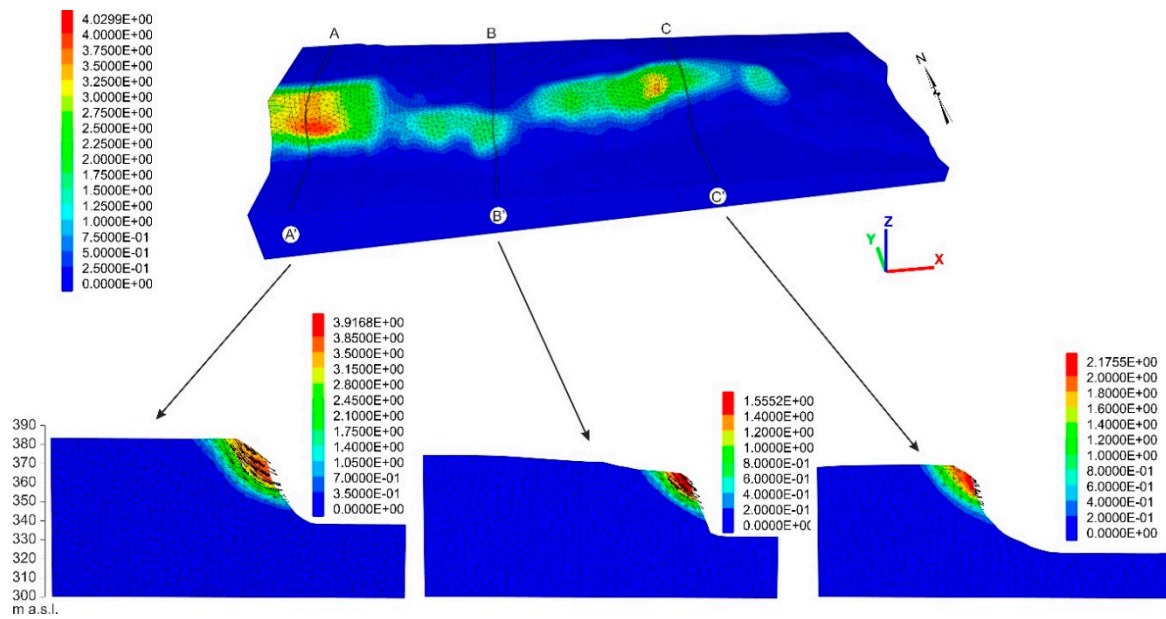


**Figure 22.** Contour displacements and displacement vectors (sections) of the pre-landslide model without discontinuities and with pore pressures.

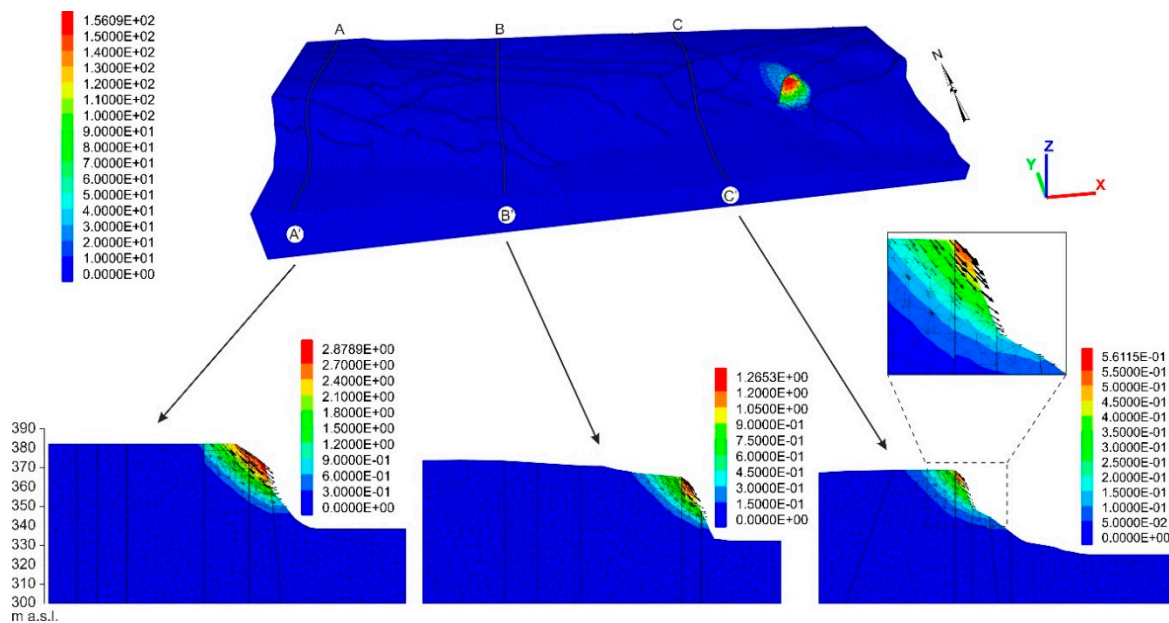


**Figure 23.** Contour displacement and displacement vectors (sections) of the post-landslide model with discontinuities.

### Post-Landslide Dynamic Analysis of the Model with Discontinuities

The dynamic analysis was also performed on the complete post-landslide model (with discontinuities), again introducing the chosen seismic input (the Mw 5.5 event which occurred on 18 January 2017). The area with the greatest displacements is located along main joints in the left side of the main scarp of the February 2018 landslide (Figure 24) and corresponds to the area outlined by the static analysis.

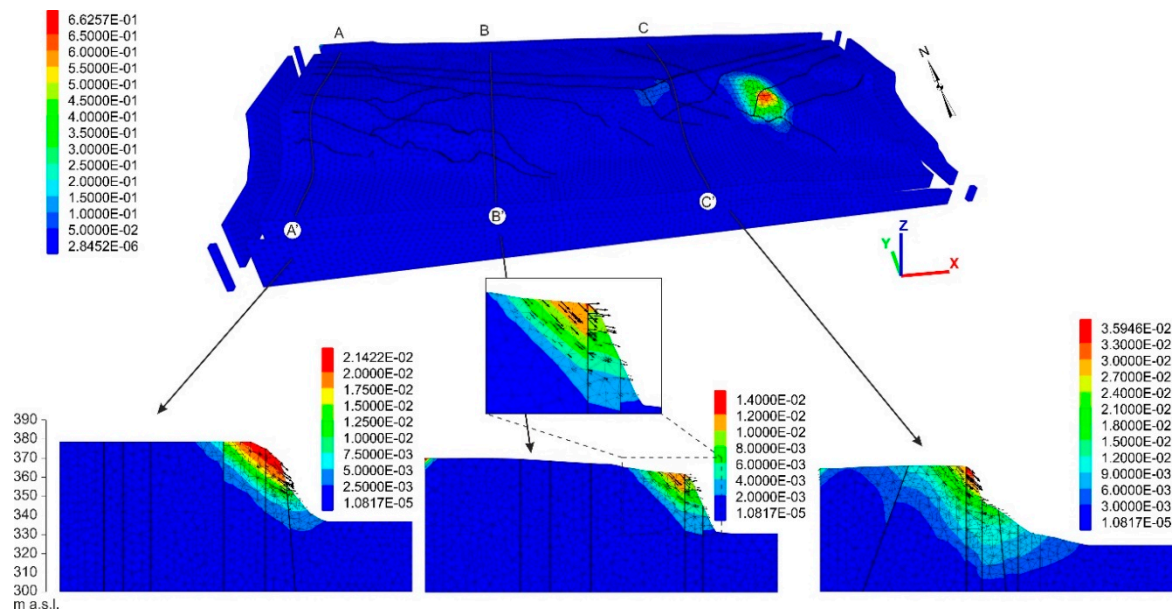


**Figure 24.** Contour displacements and displacement vectors (sections) of the dynamic analysis with Mw 5.5 input on the post-landslide model with discontinuities.

## 5. Discussion

The combination of field, remote and lab analyses (i.e., topographic, geostructural, geomorphological, photogeological) and 3D simulation modelling allowed for the characterization of the Ponzano landslide and the Castelnuovo landslide (NE-Abruzzo hilly area, Central Italy), which occurred in February 2017 after >1 month of heavy snowfall and rainfall and after January 2017 Mw > 5 earthquakes.

The Ponzano landslide affected a NNW–SSE oriented hog-back on alternated arenaceous and pelitic-arenaceous Miocene–Pliocene rocks with a thick cover of colluvial deposits and previous landslide deposits. It is a composite landslide incorporating several sliding blocks, mostly due to translational sliding movements with a rotational component in the upper part and evolving to flow in the lower part. The development of the landslide scarp system is highly controlled by the hog-back arrangement. Translational movement documented by push ridges and groves on the slip surfaces affects the lateral scarps. Sets of minor scarps and tension cracks outline the sliding blocks. The landslide involved the colluvial cover and also the upper part of the bedrock. The trigger occurred around one month after the last Mw  $\geq 5$  seismic event, a few days after the closest rainfall event and after >1 month of heavy snowfall and during snowmelt connected to temperature rise.

The deformation occurred mostly on 12 February 2017 and in the next few days. The total recorded slip is up to 15–18 m in the upper and middle parts of the landslide and decreases to zero in the northern and in the lower parts. Comparing our displacement analysis with previous investigations [22,23], it is possible to infer the deformation pattern occurred in the Ponzano landslide and its rate. In the upper part close to the main scarps, the landslide shows the highest deformation (up to 18 m); the deformation decreases in the central part (up to 10–14 m) and increases again in the middle-lower part (downstream Villa Carosi); finally, in the lower part the deformation decreases to zero. The deformation rates can only be estimated comparing all the available data and field observation to the previous studies [22,23]. Since the deformation detected before 12 February 2017 is very slow (i.e., up to 3 cm/year on average [22]) and the deformation after 23 February 2017 is also slow (up to 65 cm in 5 months, 13 cm/month on average and maximum 10 cm/day [23]), most of the deformation has occurred in a 10-days' time span (12–22 February). Comparing field observation and remote data is possible to infer a movement up to 0.5–1 m/h in the first day and slower, at <1 m/day, in the next few days, accomplishing the total translational movement of up to 15–18 m toward the ESE.

The Castelnuovo landslide involved a mesa relief consisting of a ~60–70 m-thick layer of Middle Pleistocene alluvial fan conglomerate-sandstone rocks bounded by a 30–60 m-high polygenetic scarp. Both the relief and the scarp are affected by WNW–ESE and WSW–ENE oriented main joints (consistent with the regional main geomorphological evidence of tectonics [51]) defining a geological model consisting of a system of conglomerate-sandstone polygonal wedges. The analysis outlined that the landslide occurred at the intersection of the main joints; the landslide mechanism is due to topple/fall of the outer wedges on the slope combined with slide or collapse of the inner wedges bounded by major joints. As in the Ponzano case, the trigger occurred around one month after the last  $M_w \geq 5$  seismic event, a few days from the closest rainfall event, after >1 month of heavy snowfall and during snowmelt due to temperature rise.

The comparison of geological and geomorphological results with the 3D numerical modelling, performed with the aim of evaluating the main factor controlling the landsliding of the slope, showed that:

- the occurrence of two systems of major joints trending WNW–ESE and WSW–ENE controlled the location, geometry and mechanism of the February 2017 landslide; the distribution of the instability areas along the entire Castelnuovo slope is at the intersection of the main joints, where only minor landslides occurred so far; the post-landslide modelling confirms the instability areas outlining again the most critical one at the intersection of the main joints systems with the main landslide scarp;
- seismic shaking is not found to be a possible triggering factor for the landslide; however, it could have worsened the slope stability, acting as a predisposing factor for rainfall-snowmelt induced landsliding (as largely documented worldwide; e.g., [6]).
- snowfall and melting—worsened by poor water drainage on top of Castelnuovo relief—inducing pore pressure increase in the upper part of the slope are found to be the main triggering factor for this landslide.

Moreover, the numerical modelling (both pre- and post-landslide) outlined other sectors of the scarp in critical stability conditions, which may affect the houses at the top of the scarp and allowed the effective evaluation of the safety and civil protection procedure and more widely to assess the landslide risk mitigation of Castelnuovo village.

## 6. Concluding Remarks

In January and February 2017, several landslides occurred in the NE-Abruzzo piedmont hilly area after a meteorological event with heavy snowfall and rainfall (January 2017) combined with moderate seismic shaking (the last events of the 2016–2017 Central Italy seismic crisis occurred on 18 January 2017, with  $M_w \geq 5$ ). Through a combination of field, remote and lab analyses with 3D simulation modelling, we investigated two case studies occurred in mid-February: the Ponzano landslide and the Castelnuovo landslide (NE-Abruzzo, Central Italy). These cases are representative of the landslides affecting the piedmont hills of NE-Abruzzo developed on weak rocks (e.g., pelitic-arenaceous rocks, conglomerate-sandstone rocks). This study allowed to provide a contribution in the comprehension of the role of the morphostructural setting and seismic and meteorological factors in the development of landslides in weak rocks.

In summary, the main landslides, that affected weak rocks hills in this area, are controlled by:

- the lithology and morphostructural setting (e.g., hog-back relief, mesa relief affected by intersecting major joints) as a predisposing factor for the shape of the landslide scarp and geometry of the landslide (e.g., following the hog-back setting in Ponzano and the intersection of the main joints in Castelnuovo), as well as in the kinematics of the sliding (e.g., topple and sliding following the main joints in the Castelnuovo landslide);
- the seismic shaking, which affected the area during the 2016–2017 Central Italy seismic crisis is not found to have triggered the landslides but seems to have contributed to worsening the

stability conditions of the slope acting as a predisposing factor; delayed landslides were triggered by other events (e.g., meteorological), as largely documented worldwide;

- the meteorological events, which affected the area in January–February 2017 (heavy snowfall and rainfall events followed by snowmelt), are found to be the main triggering cause (i.e., inducing the increase of pore water pressure in the slopes).

This integrated study outline how detailed geological and geomorphological field survey combined with remote UAV investigation, borehole analysis, photogeological interpretation and with numerical modelling for stability analysis, provides an effective approach in the analysis of the landslides. This is particularly true in areas, like the eastern piedmont-hilly area of the Apennines, which are largely affected by meteorological events and seismicity inducing a large distribution of landslides. This approach provides an effective base for the definition of the 3D model of landslides and for the correct monitoring as well as for pre- and post-landslide hazard-risk assessment.

**Author Contributions:** Funding acquisition, N.S.; Conceptualization and Methodology, E.M. and N.S.; Investigation, M.C. and T.P.; Software, M.C. and N.S.; Supervisions E.M. and N.S.; Writing—Original draft, M.C. and T.P.; Writing—Final version, N.S., E.M., M.C. and T.P.

**Funding:** This research and the APC was funded by Nicola Sciarra, grant provided by Civil Protection Office of Abruzzo Region.

**Acknowledgments:** The authors wish to thank the Abruzzo Civil Protection Office and the Municipalities of Campli and Civitella del Tronto for providing access to the landslide areas, logistic and data support. The authors wish also to thank the Cartographic Office of Abruzzo Region by means of the Open Geodata Portal (<http://opendata.regione.abruzzo.it/>), for providing the topographic data, aerial photos and orthophotos used for this work. A special thank goes to the anonymous reviewers and to the Academic Editor, whose precious comments and suggestion helped us to largely improve the manuscript and the figures.

**Conflicts of Interest:** The authors declare no conflict of interest.

## References

1. Trigila, A.; Iadanza, C.; Bussettini, M.; Lastoria, B. *Dissesto Idrogeologico in Italia: Pericolosità e Indicatori di Rischio, Edizione 2018*; ISPRA Rapporti 287; ISPRA: Rome, Italy, 2018; pp. 1–172.
2. Canuti, P.; Casagli, N.; Ermini, L.; Fanti, R.; Farina, P. Landslide activity as a geoindicator in Italy: Significance and new perspectives from remote sensing. *Environ. Geol.* **2004**, *45*, 907–919. [[CrossRef](#)]
3. Carrara, A.; Crosta, G.; Frattini, P. Geomorphological and historical data in assessing landslide hazard. *Earth Surf. Proc. Land.* **2003**, *28*, 1125–1142. [[CrossRef](#)]
4. Segoni, S.; Piciullo, L.; Gariano, S.L. A review of the recent literature on rainfall thresholds for landslide occurrence. *Landslides* **2018**, *15*, 1–19. [[CrossRef](#)]
5. Segoni, S.; Rosi, A.; Rossi, G.; Catani, F.; Casagli, N. Analysing the relationship between rainfalls and landslides to define a mosaic of triggering thresholds for regional-scale warning systems. *Nat. Hazards Earth Syst. Sci.* **2014**, *14*, 2637–2648. [[CrossRef](#)]
6. Zhang, S.; Zhang, L.M.; Glade, T. Characteristics of earthquake- and rain-induced landslides near the epicenter of Wenchuan earthquake. *Eng. Geol.* **2014**, *175*, 58–73. [[CrossRef](#)]
7. Glade, T.; Crozier, M.J. Landslide geomorphology in a changing environment. *Geomorphology* **2010**, *120*, 1–2. [[CrossRef](#)]
8. Gariano, S.L.; Guzzetti, F. Landslides in a changing climate. *Earth Sci. Rev.* **2016**, *162*, 227–252. [[CrossRef](#)]
9. Alvioli, M.; Melillo, M.; Guzzetti, F.; Rossi, M.; Palazzi, E.; von Hardenberg, J.; Brunetti, M.T.; Peruccacci, S. Implications of climate change on landslide hazard in Central Italy. *Sci. Total Environ.* **2018**, *630*, 1528–1543. [[CrossRef](#)]
10. Bozzano, F.; Gambino, P.; Prestininzi, A.; Scarascia Mugnozza, G.; Valentini, G. Ground effects induced by the Umbria-marche earthquakes of September–October 1997, Central Italy. In Proceedings of the 8th International Congress of International Association for Engineering Geology and the Environment, Vancouver, Canada, 21–25 September 1998; Volume, 2, pp. 825–830.
11. Keefer, D.K. Landslides caused by earthquakes. *Geol. Soc. Am. Bull.* **1984**, *95*, 406–421. [[CrossRef](#)]

12. Romeo, R.W. Seismically induced landslide displacements: A predictive model. *Eng. Geol.* **2000**, *58*, 337–351. [[CrossRef](#)]
13. Peruccacci, S.; Brunetti, M.T.; Luciani, S.; Vennari, C.; Guzzetti, F. Lithological and seasonal control on rainfall thresholds for the possible initiation of landslides in central Italy. *Geomorphology* **2012**, *139–140*, 79–90. [[CrossRef](#)]
14. Sacchini, A.; Faccini, F.; Ferraris, F.; Firpo, M.; Angelini, S. Large-scale landslide and deep-seated gravitational slope deformation of the Upper Scrivia Valley (Northern Apennine, Italy). *J. Maps* **2016**, *12*, 344–358. [[CrossRef](#)]
15. Vanneschi, C.; Eyre, M.; Francioni, M.; Coggan, J. The Use of Remote Sensing Techniques for Monitoring and Characterization of Slope Instability. *Procedia Eng.* **2017**, *191*, 150–157. [[CrossRef](#)]
16. Francioni, M.; Salvini, R.; Stead, D.; Coggan, J. Improvements in the integration of remote sensing and rock slope modeling. *Nat. Hazards* **2018**, *90*, 975–1004. [[CrossRef](#)]
17. Regione Abruzzo. Calamità Naturali. Available online: <https://www.regione.abruzzo.it/content/calamitanaturali> (accessed on 10 August 2018).
18. Di Lena, B.; Giuliano, D. Report Meteorologico del Mese di Gennaio e Febbraio 2017 Nella Regione Abruzzo. Available online: <https://docplayer.it/54882937-Report-meteorologico-del-mese-di-gennaio-2017-nella-regione-abruzzo.html> (accessed on 7 March 2019).
19. Chiaraluce, L.; Di Stefano, R.; Tinti, E.; Scognamiglio, L.; Michele, M.; Casarotti, E.; Cattaneo, M.; De Gori, P.; Chiarabba, C.; Monachesi, G.; et al. The 2016 central Italy seismic sequence: A first look at the mainshocks, aftershocks, and source models. *Seismol. Res. Lett.* **2017**, *88*, 757–771. [[CrossRef](#)]
20. National Institute of Geophysics and Volcanology (INGV). ISIDE Working Group (2018) Version 1.0. Available online: <http://cnt.rm.ingv.it/> (accessed on 3 August 2018). [[CrossRef](#)]
21. Piacentini, T.; Galli, A.; Marsala, V.; Miccadei, E. Analysis of Soil Erosion Induced by Heavy Rainfall: A Case Study from the NE Abruzzo Hills Area in Central Italy. *Water* **2018**, *10*, 1314. [[CrossRef](#)]
22. Solari, L.; Raspini, F.; Del Soldato, M.; Bianchini, S.; Ciampalini, A.; Ferrigno, F.; Tucci, S.; Casagli, N. Satellite radar data for back-analyzing a landslide event: The Ponzano (Central Italy) case study. *Landslide* **2018**, *15*, 773–782. [[CrossRef](#)]
23. Allasia, P.; Baldo, M.; Giordan, D.; Godone, D.; Wrzesniak, A.; Lollino, G. Near Real Time Monitoring Systems and Periodic Surveys Using a Multi Sensors UAV: The Case of Ponzano Landslide. In Proceedings of the IAEG/AEG Annual Meeting, San Francisco, CA, USA, 17–21 September 2018; Springer International Publishing: Cham, Switzerland, 2018; Volume 1, pp. 303–310.
24. Di Francesco, R.; Siena, M.; Tiberii, M.G.; Labagnara, R.; Di Matteo, L.; Scaletta, G. Il contributo della geotecnica nella comprensione dei dissesti storici dell’Abitato di Campli (TE). In Proceedings of the XXII Convegno Nazionale di Geotecnica, Palermo, Italy, 16–18 May 2007.
25. D’Alessandro, L.; Miccadei, E.; Piacentini, T. Morphostructural elements of central-eastern Abruzzi: Contributions to the study of the role of tectonics on the morphogenesis of the Apennine chain. *Quat. Int.* **2003**, *101–102*, 115–124. [[CrossRef](#)]
26. Progetto IFFI (Inventario dei Fenomeni Franosi in Italia) ISPRA-Dipartimento Difesa del Suolo-Servizio Geologico d’Italia-Regione Abruzzo. Available online: <http://www.progettoiffi.isprambiente.it/cartanetiffi/> (accessed on 1 December 2018).
27. Marchetti, D.; D’Amato Avanzi, G.; Sciarra, N.; Calista, M. Slope stability modeling of a sandstone cliff south of Livorno (Tuscany, Italy). In *Risk Analysis VI Simulation and Hazard Mitigation, Proceedings of the 6th International Conference on Computer Simulation Risk Analysis and Hazard Mitigation, Cephalonia, Greece, 5–7 May 2008*; Brebbia, C.A., Beriatos, E., Eds.; WitPress: Southampton, UK, 2008; pp. 321–333.
28. Sciarra, N.; Miccadei, E.; Calista, M.; Marchetti, D. Distinct element analysis of jointed and karstified rocks in a former quarry. In *Rock Engineering in Difficult Ground Conditions—Soft Rocks and Karst, Proceedings of the Regional Symposium of the International Society for Rock Mechanics EUROCK 2009, Dubrovnik, Cavtat, Croatia, 29–31 October 2009*; Vrkljan, I., Ed.; Leiden CRC Press: Taylor & Francis Group: London, UK, 2010; pp. 507–512.
29. Sciarra, N.; Calista, M.; Pasculli, A.; Mataloni, G. Numerical modeling and hazard of a cliff in anthropic and historical contexts. In *ISRM International Symposium-EUROCK 2016; International Society for Rock Mechanics and Rock Engineering: Ürgüp-Nevşehir, Turkey, 2016*.

30. Aringoli, D.; Calista, M.; Gentili, B.; Pambianchi, G.; Sciarra, N. Geomorphological features and 3d modeling of Montelparo mass movement (Central Italy). *Eng. Geol.* **2008**, *99*, 70–84. [[CrossRef](#)]
31. Marchetti, D.; D'amato Avanzi, G.; Pochini, A.; Puccinelli, A.; Sciarra, N.; Calista, M. Geomechanical characterization and 3d numerical modeling of complex rock masses: A study case in Italy. In *ISRM International Symposium on Rock Mechanics-SINOROCK2009-“Rock Characterization, Modeling and Engineering Design Methods”*; International Society for Rock Mechanics and Rock Engineering: Hong Kong, China, 2009; pp. 216–220.
32. Pasculli, A.; Sciarra, N.; Esposito, L.; Esposito, A.W. Effects of wetting and drying cycles on mechanical properties of pyroclastic soils. *Catena* **2017**, *156*, 113–123. [[CrossRef](#)]
33. Pasculli, A.; Audisio, C. Cellular Automata Modelling of Fluvial Evolution: Real and Parametric Numerical Results Comparison along River Pellica (NW Italy). *Environ. Model. Assess.* **2015**, *20*, 425–441. [[CrossRef](#)]
34. Pasculli, A.; Sciarra, N. A probabilistic approach to determine the local erosion of a watery debris flow. In *Proceedings of the XI IAEG International Congress*, Liege, Belgium, 3–8 September 2006.
35. Calista, M.; Pasculli, A.; Sciarra, N. Reconstruction of the geotechnical model considering random parameters distributions. *Eng. Geol. Soc. Territ.* **2015**, *2*, 1347–1351.
36. Pasculli, A.; Calista, M.; Sciarra, N. Variability of local stress states resulting from the application of Monte Carlo and finite difference methods to the stability study of a selected slope. *Eng. Geol.* **2018**, *245*, 370–389. [[CrossRef](#)]
37. Pasculli, A.; Minatti, L.; Sciarra, N. Insights on the application of some current SPH approaches for the study of muddy debris flow: Numerical and experimental comparison. In *Wit Transaction on Information and Communication Technologies, Proceedings of the 10th International Conference on Advances in Fluid Mechanics, AFM 2014, Coruna, Spain, 1 July 2014*; WIT Press: Ashurst, UK, 2014; Volume 82, pp. 3–14.
38. Jiang, J.; Ehret, D.; Xiang, W.; Rhon, J.; Huang, L.; Yan, S.; Bi, R. Numerical simulation of Qiaotou Landslide deformation caused by drawdown of the Three Gorges Reservoir, China. *Environ. Earth Sci.* **2011**, *62*, 411–419. [[CrossRef](#)]
39. Cała, M.; Flisiak, J.; Tajduś, A. Slope stability analysis with FLAC In 2D and 3D. In *Proceedings of the 4th International FLAC Symposium on Numerical Methods in Geomechanics*, Madrid, Spain, 29–31 May 2006; pp. 11–14.
40. Shen, H.; Klapperich, H.; Abbas, S.M.; Ibrahim, A. Slope stability ananlisys based on the integration of GIS and numerical simulation. *Autom. Constr.* **2012**, *26*, 46–53. [[CrossRef](#)]
41. Zhang, Y.; Zhang, J.; Chen, G.; Zheng, L.; Li, Y. Effects of vertical seismic force on initiation of the Daguangbao landslide induced by the 2008 Wenchuan earthquake. *Soil Dyn. Earthq. Eng.* **2015**, *73*, 91–102. [[CrossRef](#)]
42. Islam, S.; Abdullah, R.A.B.; Mallick, J. Static and dynamic analysis of mansa devi hill landslide using flac3D. *Int. J. Civ. Eng. Technol. (IJCIET)* **2017**, *8*, 631–643.
43. Patacca, E.; Scandone, P.; Di Luzio, E.; Cavinato, G.P.; Parotto, M. Structural architecture of the central Apennines: Interpretation of the CROP 11 seismic profile from the Adriatic coast to the orographic divide. *Tectonics* **2008**, *27*, TC3006. [[CrossRef](#)]
44. Parotto, M.; Cavinato, G.P.; Miccadei, E.; Tozzi, M. Line CROP 11: Central Apennines. In *CROP Atlas: Seismic Reflection Profiles of the Italian Crust*; Scrocca, D., Doglioni, C., Innocenti, F., Manetti, P., Mazzotti, A., Bertelli, L., Burbi, L., D'Offizi, S., Eds.; Istituto Superiore per la Protezione e la Ricerca Ambientale: Roma, Italy. Available online: <http://www.isprambiente.gov.it/en/publications/technical-periodicals/descriptive-memories-of-the-geological-map-of/crop-atlas-seismic-reflection-profiles-of-the> (accessed on 10 September 2018).
45. Miccadei, E.; Piacentini, T.; Buccolini, M. Long-term geomorphological evolution in the Abruzzo area (Central Apennines, Italy): Twenty years of research. *Geol. Carpath. Carpathica* **2017**, *68*, 19–28. [[CrossRef](#)]
46. Piacentini, T.; Miccadei, E. The role of drainage systems and intermontane basins in the Quaternary landscape of the Central Apennines chain (Italy). *Rend. Lincei* **2014**, *25*, 139–150. [[CrossRef](#)]
47. Regione Abruzzo. Modello Digitale del Terreno-Risoluzione 10 × 10 Metri. Available online: [http://opendata.regione.abruzzo.it/opendata/Modello\\_digitale\\_del\\_terreno\\_risoluzione\\_10x10\\_metri](http://opendata.regione.abruzzo.it/opendata/Modello_digitale_del_terreno_risoluzione_10x10_metri) (accessed on 10 February 2019).
48. Santo, A.; Ascione, A.; Di Crescenzo, G.; Miccadei, E.; Piacentini, T.; Valente, E. Tectonic-geomorphological map of the middle Aterno River valley (Abruzzo, Central Italy). *J. Maps* **2014**, *10*, 365–378. [[CrossRef](#)]

49. Miccadei, E.; Mascioli, F.; Ricci, F.; Piacentini, T. Geomorphology of soft clastic rock coasts in the mid western Adriatic Sea (Abruzzo, Italy). *Geomorphology* **2019**, *324*, 72–94. [CrossRef]
50. ISPRA. Carta Geologica d'Italia alla Scala 1:50.000, Foglio 339 "Teramo". *Serv. Geol. Ital.* **2012**. Available online: [http://www.isprambiente.it/Media/carg/339\\_TERAMO/Foglio.html](http://www.isprambiente.it/Media/carg/339_TERAMO/Foglio.html) (accessed on 10 February 2019).
51. Della Seta, M.; Del Monte, M.; Fredi, P.; Miccadei, E.; Nesci, O.; Pambianchi, G.; Piacentini, T.; Troiani, F. Morphotectonic evolution of the Adriatic piedmont of the Apennines: An advancement in the knowledge of the Marche–Abruzzo border area. *Geomorphology* **2008**, *102*, 119–129. [CrossRef]
52. Miccadei, E.; Piacentini, T.; Gerbasì, F.; Daverio, F. Morphotectonic map of the Osento River basin (Abruzzo, Italy), scale 1:30,000. *J. Maps* **2012**, *8*, 62–73. [CrossRef]
53. Miccadei, E.; Piacentini, T.; Pozzo, A.D.; Corte, M.L.; Sciarra, M. Morphotectonic map of the Aventino–Lower Sangro valley (Abruzzo, Italy), scale 1:50,000. *J. Maps* **2013**, *9*, 390–409. [CrossRef]
54. Capelli, G.; Miccadei, E.; Raffi, R. Fluvial dynamics in the Castel di Sangro plain: Morphological changes and human impact from 1875 to 1992. *Catena* **1997**, *30*, 295–309. [CrossRef]
55. Ciccacci, S.; D'Alessandro, L.; Dramis, F.; Miccadei, E. Geomorphologic Evolution and Neotectonics of the Sulmona Intramontane Basin (Abruzzi, Apennine, Central Italy). *Zeitschrift. Geomorphol.* **1999**, *118*, 27–40.
56. Calista, M.; Miccadei, E.; Pasculli, A.; Piacentini, T.; Sciarra, M.; Sciarra, N. Geomorphological features of the Montebello sul Sangro large landslide (Abruzzo, Central Italy). *J. Maps* **2016**, *12*, 882–891. [CrossRef]
57. Buccolini, M.; Gentili, B.; Materazzi, M.; Piacentini, T. Late Quaternary geomorphological evolution and erosion rates in the clayey peri-Adriatic belt (central Italy). *Geomorphology* **2010**, *116*, 145–161. [CrossRef]
58. Regione Abruzzo, Piano Stralcio di Bacino per l'Assetto Idrogeologico dei Bacini di Rilievo Regionale Abruzzesi e del Bacino del Fiume Sangro. Servizio Difesa del Suolo Regione Abruzzo. (B.U.R.A. n. 8, 04.02.2005, Modification in 2010). Available online: <http://autoritabacini.regione.abruzzo.it/index.php/pai> (accessed on 15 December 2018).
59. Peel, M.C.; Finlayson, B.L.; McMahon, T.A. Updated world map of the Köppen-Geiger climate classification. *Hydrol. Earth Syst. Sci.* **2007**, *11*, 1633–1644. [CrossRef]
60. Di Lena, B.; Antenucci, F.; Mariani, L. Space and time evolution of the Abruzzo precipitation. *Ital. J. Agrometeorol.* **2012**, *1*, 5–20.
61. Mariani, L.; Parisi, S.G. Extreme rainfalls in the Mediterranean area. *Adv. Nat. Technol. Hazards* **2014**, *39*, 17–37.
62. Rovida, A.; Locati, M.; Camassi, R.; Lolli, B.; Gasperini, P. *CPTI15, the 2015 Version of the Parametric Catalogue of Italian Earthquakes*; INGV: Bologna, Italy, 2016. [CrossRef]
63. Locati, M.; Camassi, R.; Rovida, A.; Ercolani, E.; Bernardini, F.; Castelli, V.; Caracciolo, C.H.; Tertulliani, A.; Rossi, A.; Azzaro, R.; et al. *DBMI15, the 2015 Version of the Italian Macroseismic Database*; INGV: Bologna, Italy, 2016. [CrossRef]
64. Regione Abruzzo, Comune di Campli, Commissario Straordinario Ricostruzione Sisma–2016. Microzonazione Sismica di Livello 3 del Comune di Campli ai Sensi dell'Ordinanza del Commissario Straordinario n.24 Registrata il 15 Maggio 2017 al n. 1065. Relazione Finale. Di Antonio A. Cruciani D. Available online: [http://www.sisma2016abruzzo.it/index.php/11-informazioni-di-servizio/98-microzonazione-sismica-di-iii-livello/te/camp/67008\\_Camp/67008\\_Camp/67008\\_Camp.zip](http://www.sisma2016abruzzo.it/index.php/11-informazioni-di-servizio/98-microzonazione-sismica-di-iii-livello/te/camp/67008_Camp/67008_Camp/67008_Camp.zip) (accessed on 3 September 2018).
65. Rossi, G.; Tanteri, L.; Tofani, V.; Vannocci, P.; Moretti, S.; Casagli, N. Multitemporal UAV surveys for landslide mapping and characterization. *Landslides* **2018**, *15*, 1045–1052. [CrossRef]
66. Giordan, D.; Manconi, A.; Tannant, D.D.; Allasia, P. UAV: Low-cost remote sensing for high-resolution investigation of landslides. In Proceedings of the 2015 IEEE International Geoscience and Remote Sensing Symposium (IGARSS), Milan, Italy, 26–31 July 2015.
67. Casagli, N.; Frodella, W.; Morelli, S.; Tofani, V.; Ciampalini, A.; Intrieri, E.; Raspini, F.; Rossi, G.; Tanteri, L.; Lu, P. Spaceborne, UAV and ground-based remote sensing techniques for landslide mapping, monitoring and early warning. *Geoenviron. Disasters* **2017**, *4*, 1–23. [CrossRef]
68. Itasca. *Fast Lagrangian Analysis of Continua in 3-Dimension (FLAC3D V 5.01)*; Itasca Consulting Group: Minneapolis, MN, USA, 2012.

69. Luzi, L.; Pacor, F.; Puglia, R. *Italian Accelerometric Archive v 2.3*; Istituto Nazionale di Geofisica e Vulcanologia: Roma, Italy, 2017.
70. Bindi, D.; Pacor, F.; Luzi, L.; Puglia, R.; Massa, M.; Ameri, G.; Paolucci, R. Ground motion prediction equations derived from the Italian strong motion database. *Bull. Earthq. Eng.* **2011**, *9*, 1899–1920. [[CrossRef](#)]



© 2019 by the authors. Licensee MDPI, Basel, Switzerland. This article is an open access article distributed under the terms and conditions of the Creative Commons Attribution (CC BY) license (<http://creativecommons.org/licenses/by/4.0/>).